59th U.S. Rock Mechanics Geomechanics Symposium
SANTA FE 2025

Experimental investigation on multi-cluster temporary plugging fracturing in a horizontal well based on acoustic emission and distributed optical fiber monitoring

Prof. Haiyan Zhu

Team member: Marembo Micheal, Zhaopeng Zhang, Peng Zhao, Lei Tao

Chengdu University of Technology

State Key Laboratory of Oil and Gas Reservoir Geology and Exploitation

8 June 2025

Content

1. Background

- China ranks first globally in recoverable shale gas resources. The Sichuan Basin holds most of these resources with a recoverable volume of 27.5 trillion cubic meters. In 2024, its shale gas output reached 24 billion cubic meters, accounting for over 95% of the national total. It is the core area for China's shale gas production.

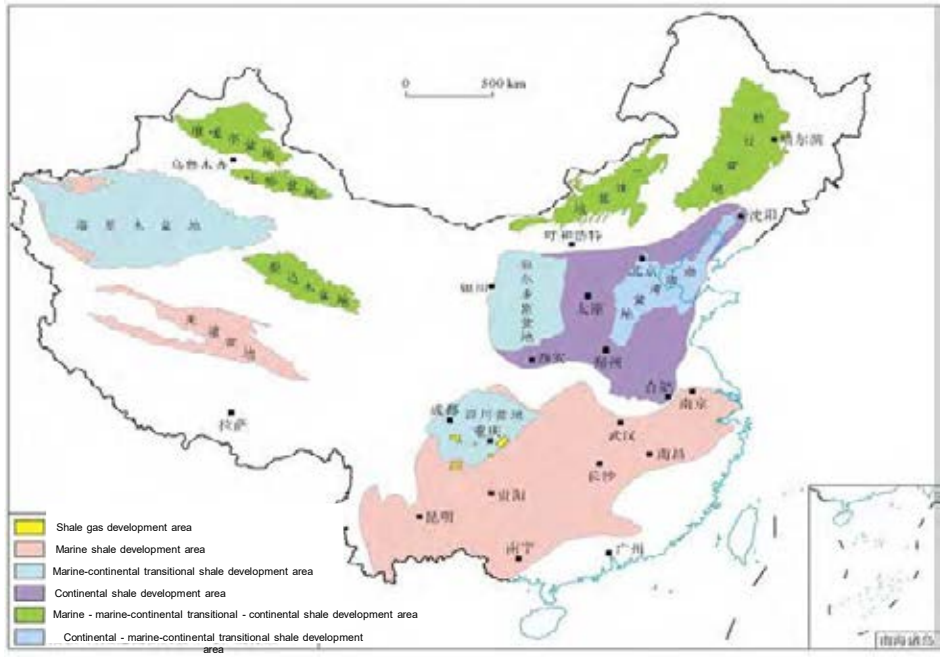

China's shale gas predominantly occurs in the Sichuan Basin's Chongqing Fuling and Changning-Weiyuan gas fields. (Guo et al., 2025)

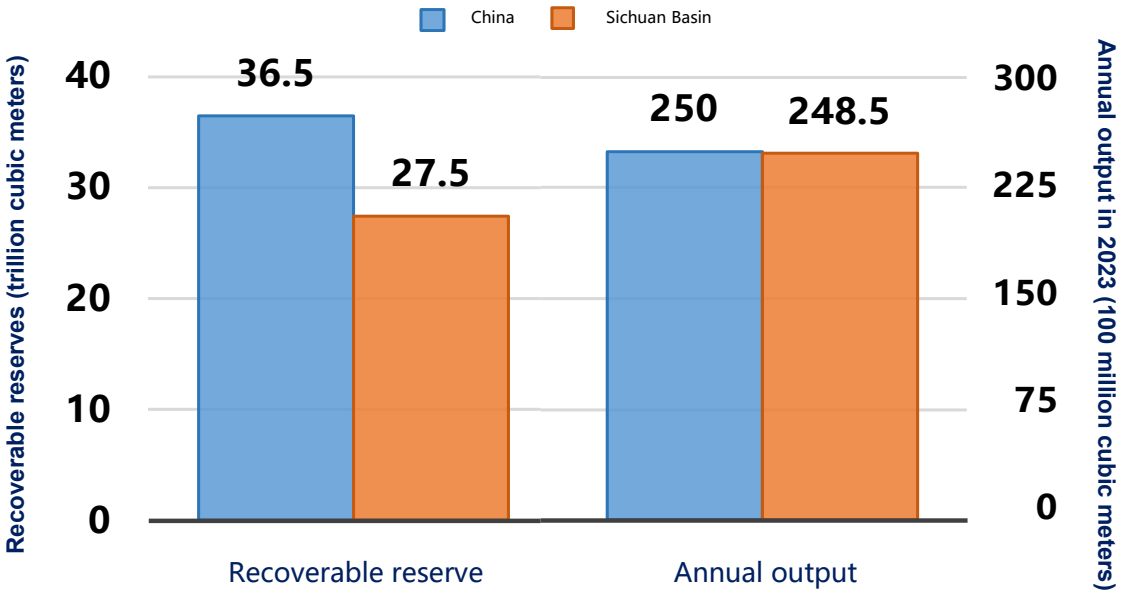

The Sichuan Basin has the highest recoverable shale gas resources and annual shale gas production in China. (National Energy Administration, 2024)

1. Background

- After more than ten years of scientific and technological research and development, China has formed a large-scale stimulation technology.
- On-site optical fiber monitoring has discovered problems such as the low initiation efficiency of perforating clusters and the difficulty in uniform propagation of multiple clusters of fractures, which seriously restricts the efficient development of shale gas.

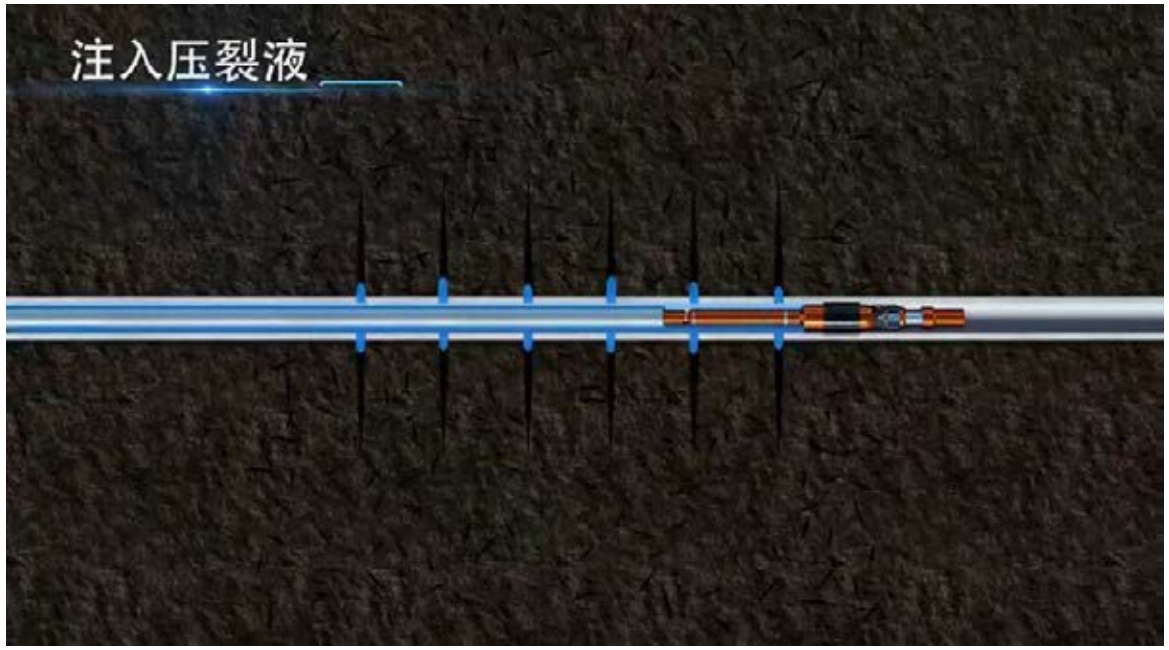

Horizontal well staged multi-cluster fracturing technology

Shale gas parameter of horizontal well cluster in China (Lei et al., 2023)

Block	horizontal section length/m	frac stage length/m	cluster spacing/m	clusters per stage
Sichuan Changning	1170-2647	59-91	6.0-11.5	6-12
Sichuan Weiyuan	1400-2253	60-130	5.7-16.4	3-17

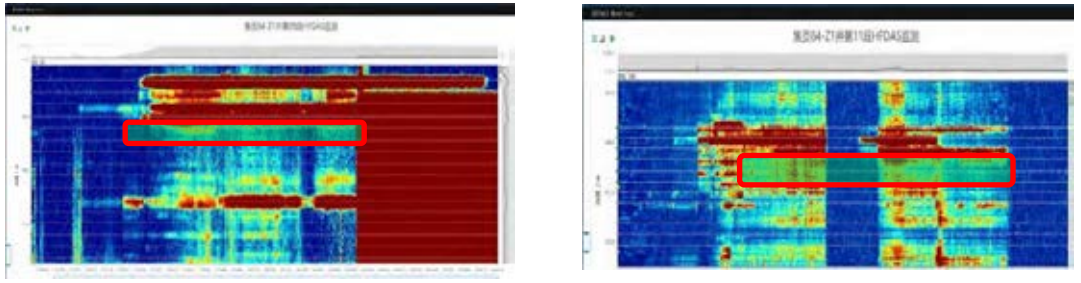

Optical fiber monitoring shows uneven multi-cluster fracture growth during shale gas development.

1. Background

- The temporary plugging fracturing (TPF) technology at the fracture opening realizes the uniform propagation of multiple clusters of fractures. However, the on-site TPF process mainly relies on engineering experience and lacks theoretical support. Especially, the position of the perforation holes that can form effective plugging and re-crack has not been clearly defined, making it difficult to support the optimization of TPF parameters.

The TPF ball is prone to sink to the bottom and fails to achieve effective blocking

Optimization of TPF parameters

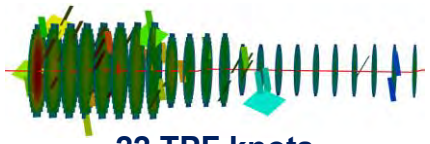

22 TPF knots

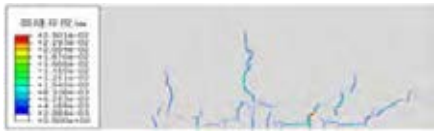

$T=30\%T_t$

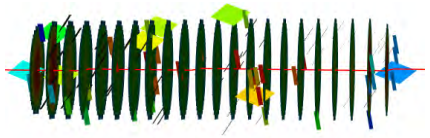

27 TPF knots

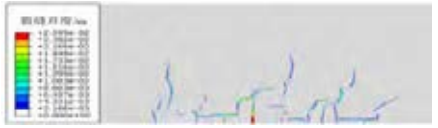

$T=40\%T_t$

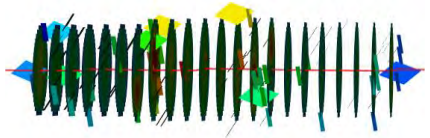

49 TPF knots

$T=50\%T_t$

1. Background

◆ To address the above-mentioned issues, **Prof. Zhu Haiyan and his team**, backed by the State Key Laboratory, has developed a true triaxial experiment system and performed physical simulations of hydraulic fracturing and fracture plugging in horizontal wells. These efforts aim to better understand fracture propagation and to provide theoretical support for promoting the uniform propagation of multiple fractures.

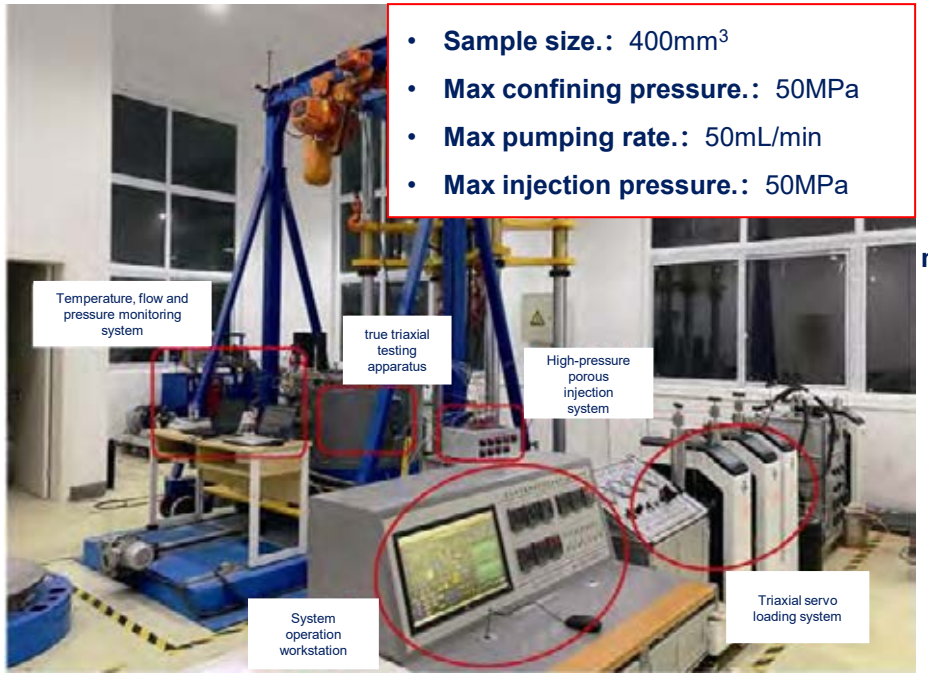

- **Sample size.:** 400mm^3
- **Max confining pressure.:** 50MPa
- **Max pumping rate.:** 50mL/min
- **Max injection pressure.:** 50MPa

A high-temperature, high-pressure, integrated drilling true triaxial physical simulation experimental system.

Multi-source monitoring

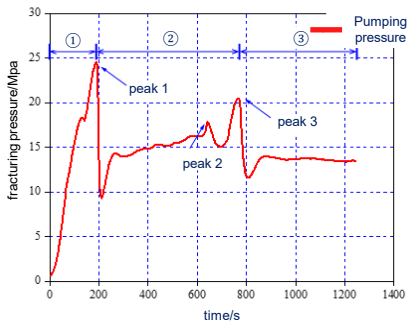

①Pressure curve

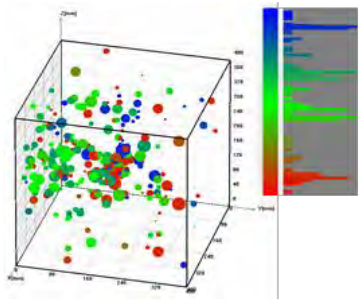

②Acoustic emission monitoring 3D positioning

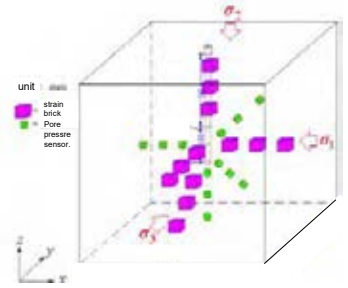

③Volumetric strain monitoring

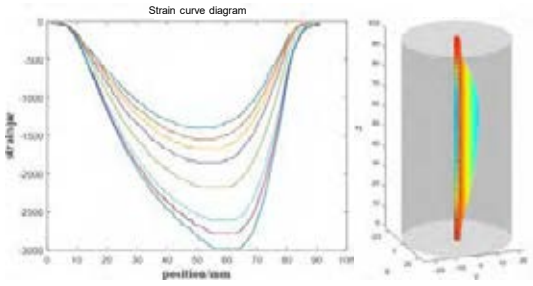

④Distributed fiber optic strain monitoring.

Content

2. Experimental Apparatus

2.1 True triaxial fracturing experimental system

- A true triaxial experiment system with multi-source monitoring for drilling, fracturing, and production was established. It can be used for physical simulation experiments on multi-cluster fracturing in a horizontal well , TPF, multi-well fracturing, and supercritical CO_2 fracturing.

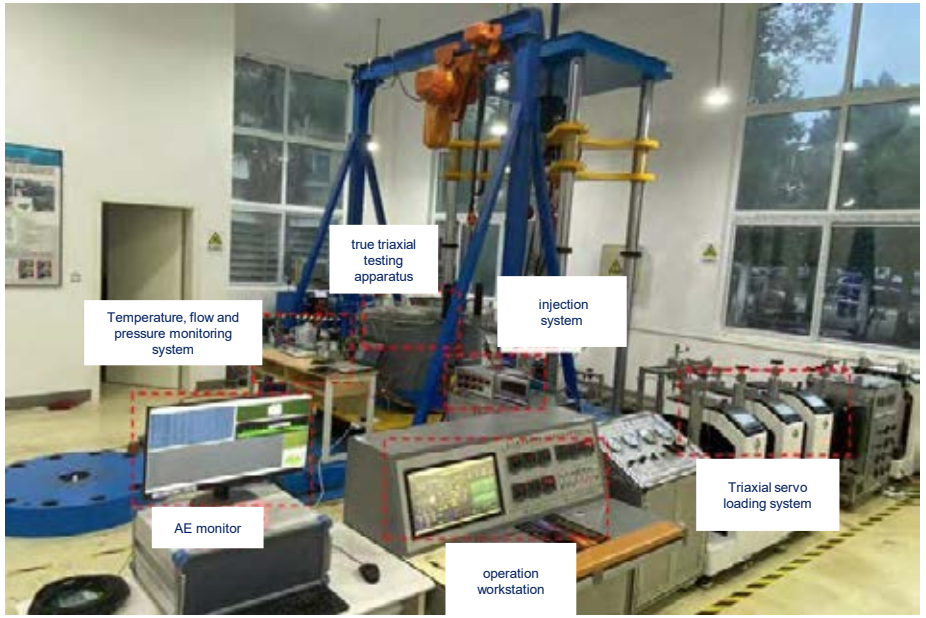

True triaxial chamber

Hydraulic pump system

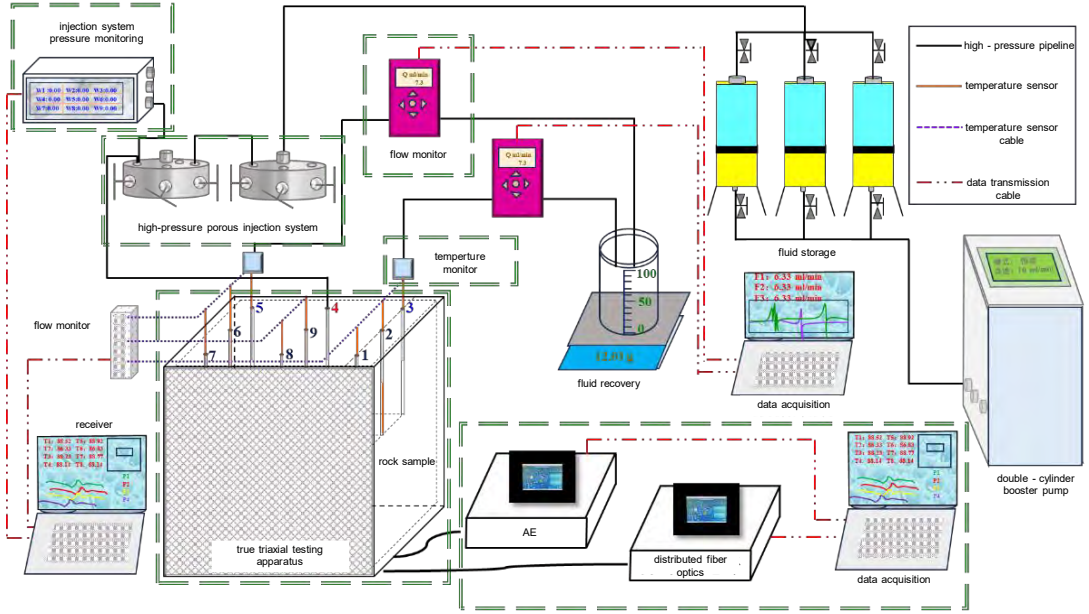

A true triaxial experimental system integrating drilling, fracturing and production with multi - source monitoring

2. Experimental Apparatus

2.2 Acoustic emission monitoring system

- A 16 channel DS5-32C acoustic emission monitoring device was developed. The continuous data transfer rate of the acoustic emission host is 262MB/s, and the waveform data transfer rate is 192MB/s.
- It is equipped with an RS-2A ceramic probe (diameter 18.8mm, height 15mm, frequency range 50 - 400KHz, center frequency 150KHz) and a gain-adjustable amplifier (bandwidth 20 - 1500KHz, maximum output voltage±10V).

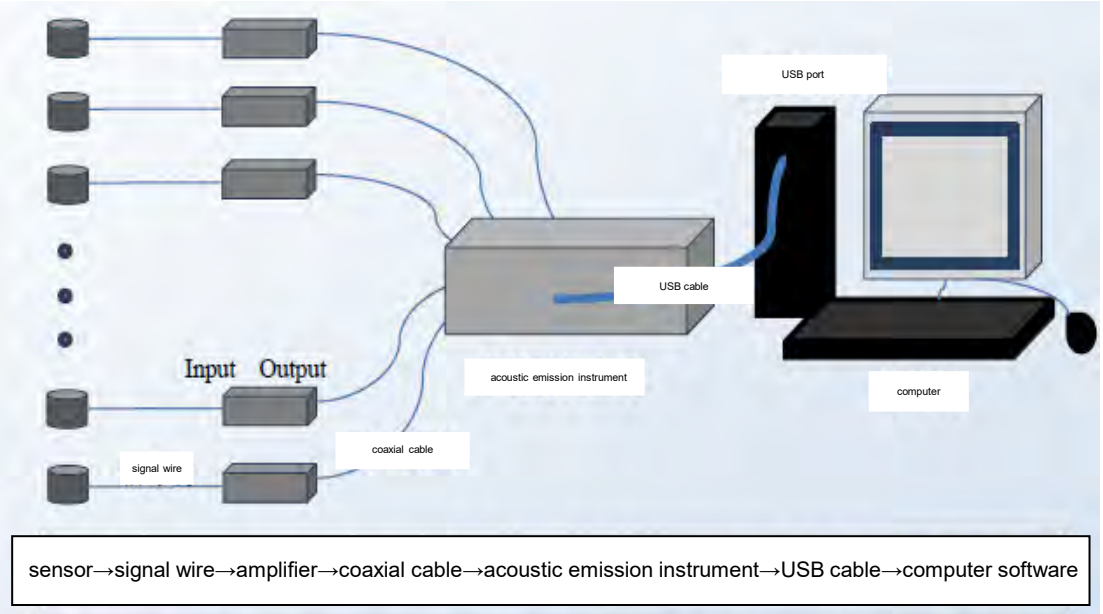

Acoustic Emission Monitoring Flow Chart

DS5-32C dynamic and static full information acoustic emission

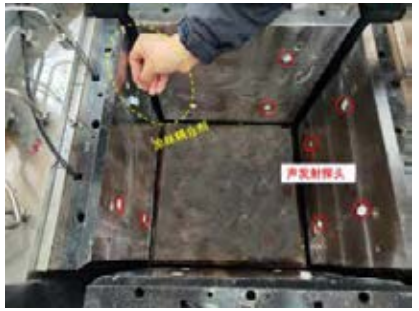

Acoustic Emission Probe Layout

Acoustic emission probes and amplifiers.

2. Experimental Apparatus

2.3 Distributed optical fiber monitoring system

- An 8 channel tShapeS-type distributed fiber-optic shape monitoring analyzer was developed. Each channel has a sensing length of ≥130m, spatial resolution of ≤0.1mm, strain measurement range of ±15000με, and strain repeatability accuracy of ±1με.
- The sensor is compatible with various fiber-optic types and high density weak-reflection fiber grating strings and has a length compensation function.

Fiber optic monitoring instrument

Fiber-optic fusion splicer

Fiber-optic cable cutter

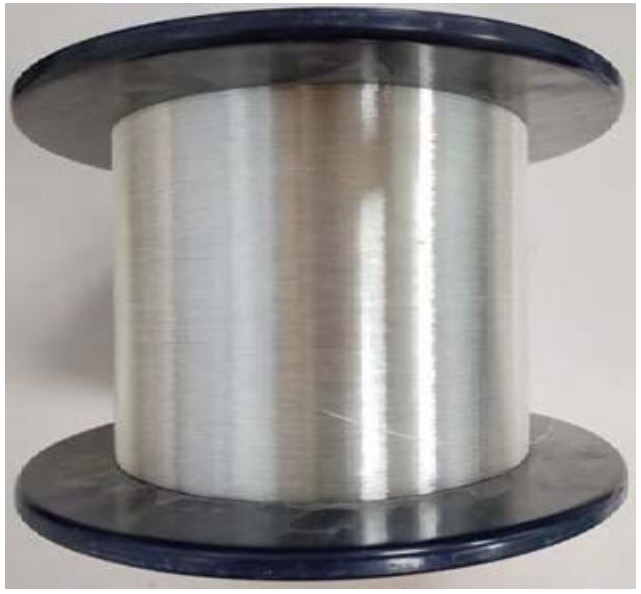

Distributed fiber optics

Content

3. Multi-cluster Propagation Experiment

- **An experimental method for multi-stage and multi-cluster fracturing propagation in horizontal wells was developed. Experiments were conducted using a true triaxial experimental system integrating drilling, fracturing and production under high-temperature and high-pressure conditions. The AE monitoring system was used to record the AE response characteristics during the fracture propagation process.**

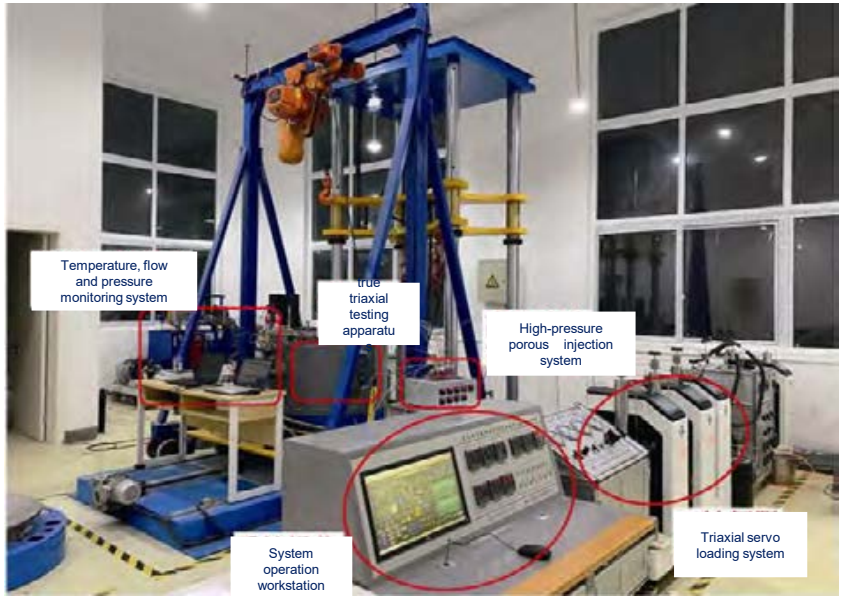

A true triaxial experimental system integrating drilling, fracturing and production with multi - source monitoring

AE monitoring system

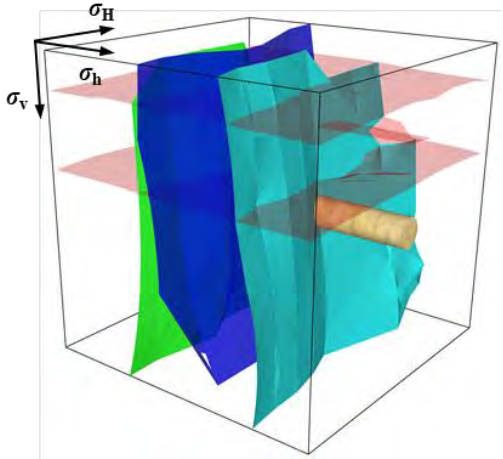

Multi-cluster fracture propagation geometries

3. Multi-cluster Propagation Experiment

3.1 Experimental Scheme

(1) Specimen Preparation

◆ The shale outcrops were processed into cubic samples of 400 × 400 × 400 mm³. The distribution of bedding planes (BPs) and natural fractures within each sample was described. At the center of each specimen, a horizontal wellbore with a diameter of 50 mm and a depth of 360 mm was drilled.

Specimen preparation

No. 1

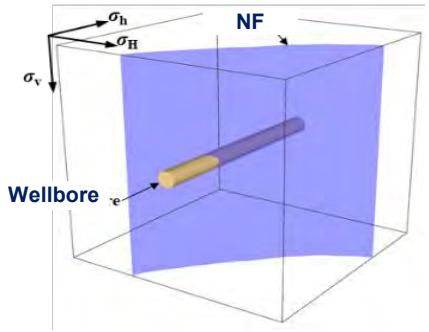

- A high-angle NF intersecting the wellboreobliquely

No. 2

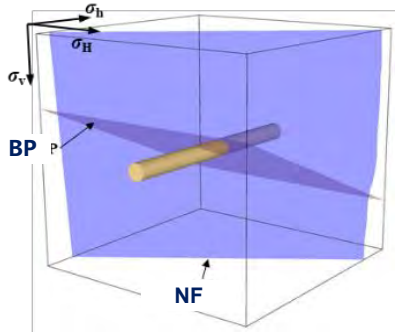

- A high-angle NF intersecting the wellbore obliquely
- An inclined BP communicating with the wellbore

No. 3

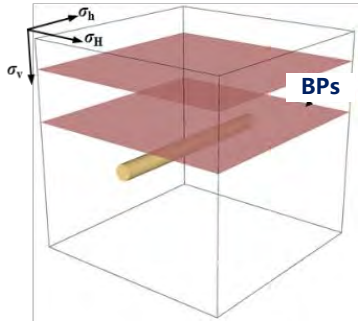

- Two BPs above the wellbore

No. 4

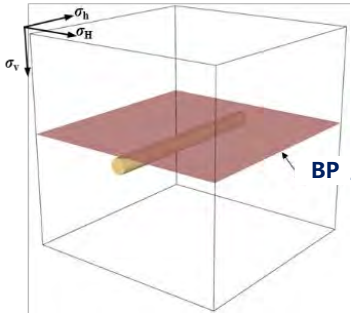

- A BP at the wellbore

No. 5

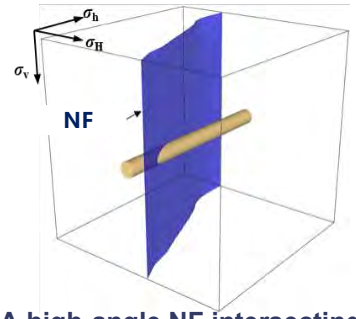

- A high-angle NF intersecting the wellbore obliquely

No. 6

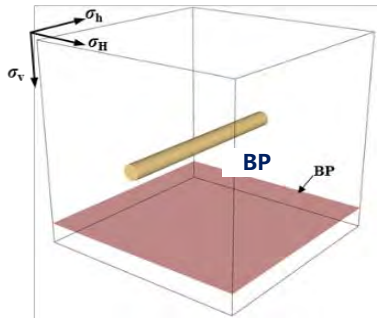

- A BP below the wellbore

3. Multi-cluster Propagation Experiment

(2) Multi-stage and multi-cluster fracturing wellbore design

- A multi-stage and multi-cluster injection wellbore was designed and fabricated. Each fracturing stage corresponds to one injection line, and the stages are isolated by steel separators to achieve segmented injection. Annular steel sheets are welded on the outer surface of the wellbore to simulate perforation clusters. Each fracturing stage is equipped with a communication tube that runs through all perforation clusters to allow for epoxy resin filling in the non-fracturing segments.

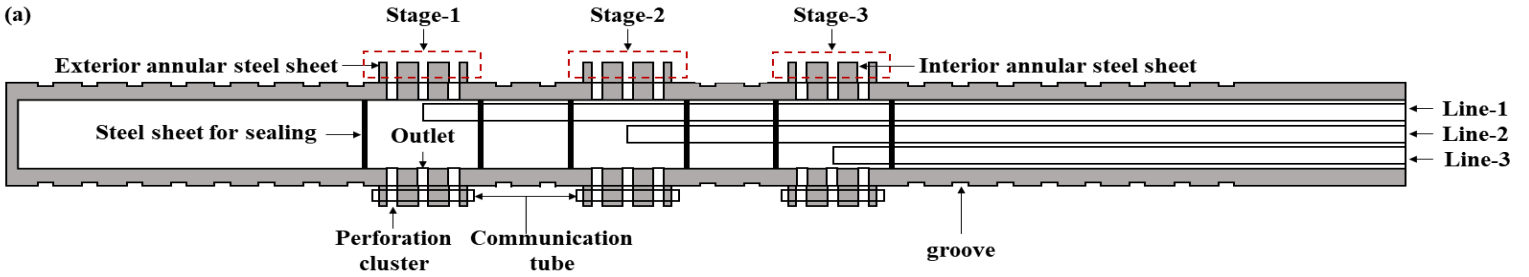

wellbore structure design

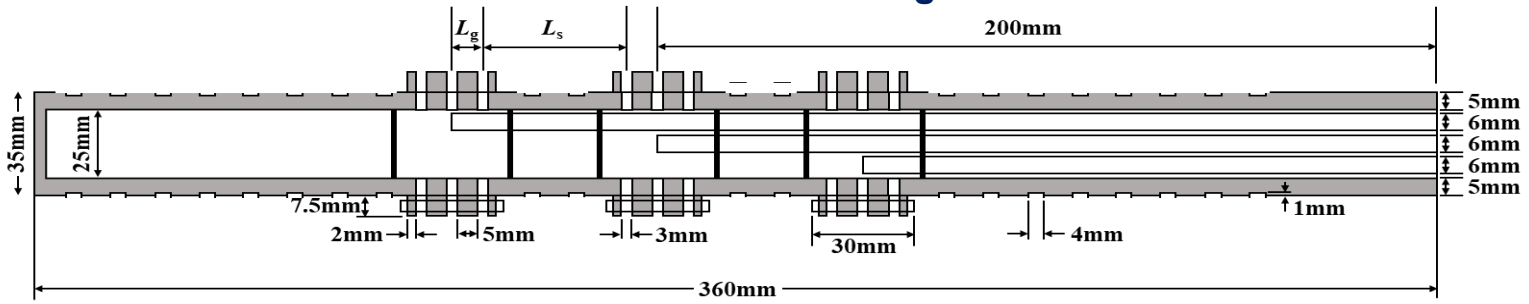

wellbore size design

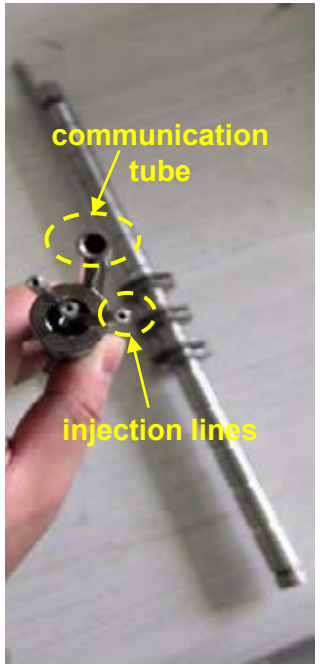

3. Multi-cluster Propagation Experiment

(3) Procedure of multi-stage and multi-cluster hydraulic fracturing experiments

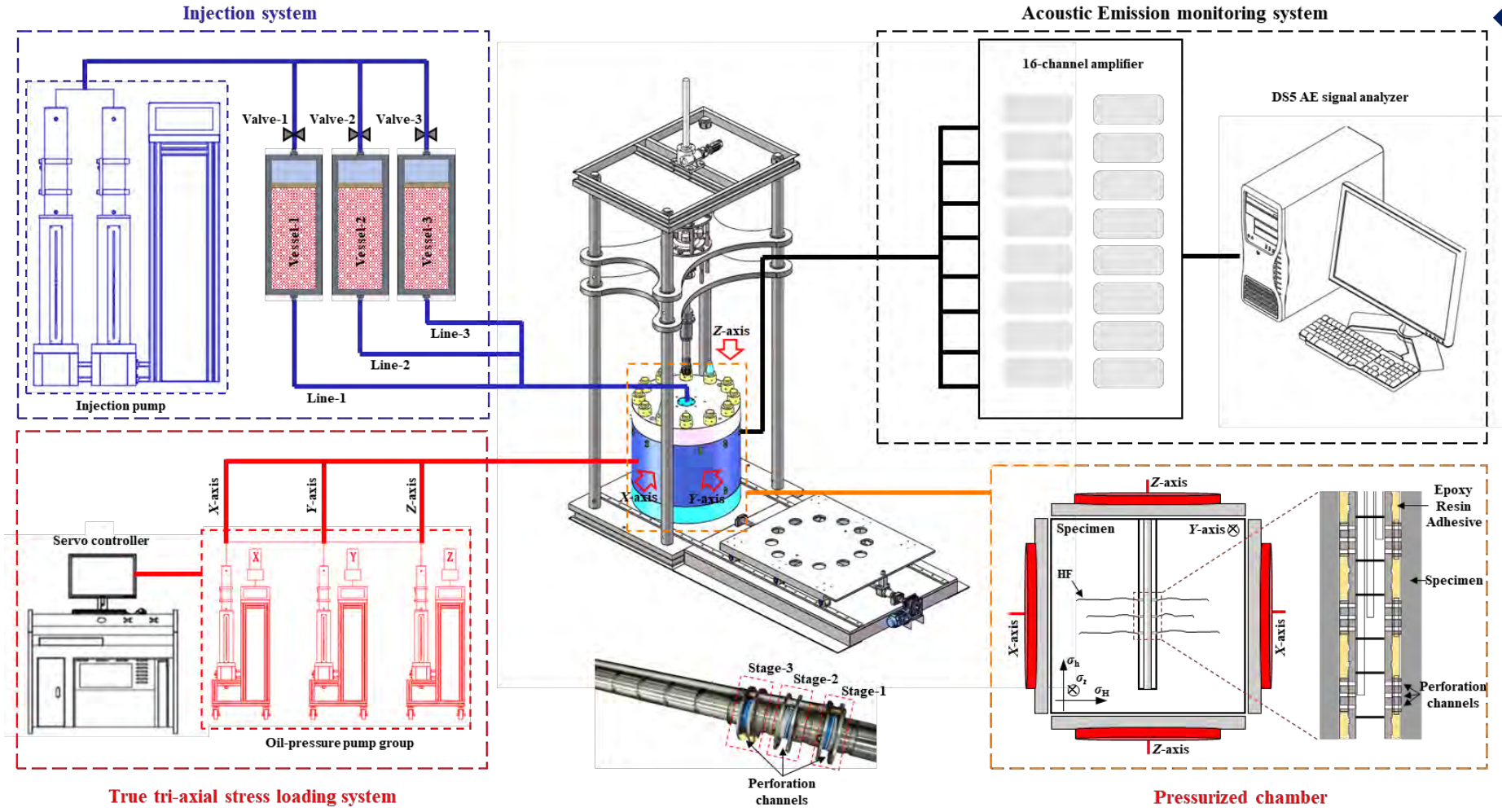

- Utilizing high-pressure lines and a six-way valve, the three injection channels are connected to their corresponding intermediate vessels. The valve of the target vessel is opened while the valves of the remaining vessels are closed. Fracturing fluid is injected into the fracturing stage at a rate of 50 mL/min, thereby achieving simultaneous and sequential fracture propagation.

Procedure of the large-scale true tri-axial multi-fracture initiation and propagation experiments

3. Multi-cluster Propagation Experiment

(4) Parameter scaling design

- Utilizing geometric scaling to design the experimental stage and cluster spacing, using horizontal and vertical stress difference coefficients to design the experimental loading stresses, and employing leak-off characteristics and dimensionless time parameters to design the fracturing fluid viscosity (200 mPa·s) and injection rate (50 mL/min), in order to achieve a similar fracture propagation regime.

Geometrical scaling (Liu et al., 2018)

$$\frac{s_M}{s_F}=\frac{L_M}{L_F}$$

Scaling of in situ stress (Beugelsdijk et al., 2000)

$$K_h=\frac{\sigma_H^F-\sigma_h^F}{\sigma_h^F}=\frac{\sigma_H^M-\sigma_h^M}{\sigma_h^M} \qquad K_v=\frac{\sigma_v^F-\sigma_h^F}{\sigma_h^F}=\frac{\sigma_v^M-\sigma_h^M}{\sigma_h^M}$$

Scaling of the HF propagation regime (Bunger et al., 2005)

$$\phi=\frac{\mu'^3E'^{11}C'^4Q}{K'^{14}} \qquad t_m=\left[\frac{\mu'^5Q^3E'^{13}}{K'^{18}}\right]^{1/2} \qquad \tau=\frac{t}{t_{mk}}$$

Experimental scheme of multi-fracture initiation and propagation in shale

No.	In situ stresses			Cluster spacing(d_c)		Stage spacing(L_c)		Number of stages and clusters	Propagation type
	σ_v/MPa	σ_H/MPa	σ_h/MPa	Field/m	Lab/mm	Field/m	Lab/mm		
1	23	25	20	16	21	-	-	1 stage; 3 clusters per stage	Simultaneous
2	23	25	20	16	21	-	-	1 stage; 3 clusters per stage	Simultaneous
3	23	25	20	-	-	25	33	3 stages; 3 cluster per stage	Sequential
4	23	25	20	-	-	25	33	3 stages; 3 cluster per stage	Sequential
5	23	25	20	8	11	40	53	3 stages; 5 cluster per stage	Simultaneous and sequential
6	23	25	20	8	11	25	33	3 stages; 6 cluster per stage	Simultaneous and sequential

Classification of HF propagation regimes

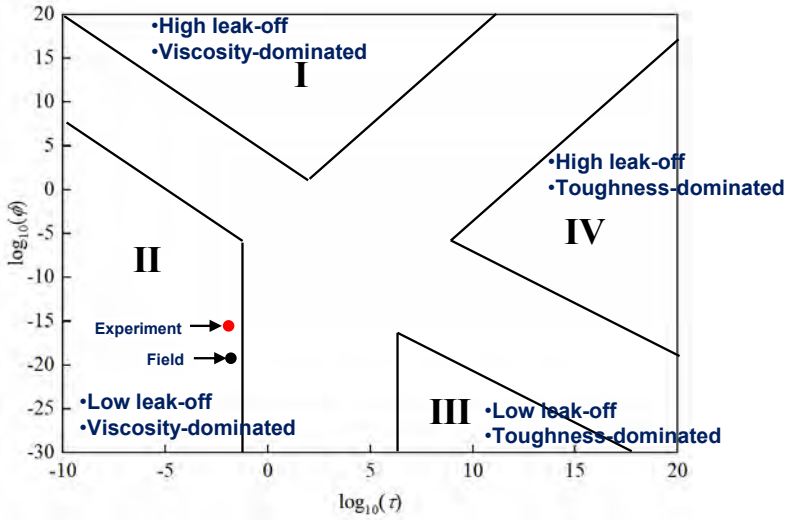

3. Multi-cluster Propagation Experiment

3.2 HF geometry and AE results of simultaneous multi-fracture propagation

(1) Specimen 1#

Parameter: σ_V=23MPa, σ_H=25MPa, σ_h=20MPa, d_c=21mm, Q=50mL/min

- A single longitudinal fracture propagating through the upper part of the specimen is formed after fracturing, with local diversions induced by NFs. The fracturing fluid primarily gathers at the toe of the horizontal wellbore, while a small amount of fluid is observed near the heel. It is suggested that the longitudinal fracture fully propagates near the toe of the horizontal wellbore, resulting in a larger width compared to that at the heel.

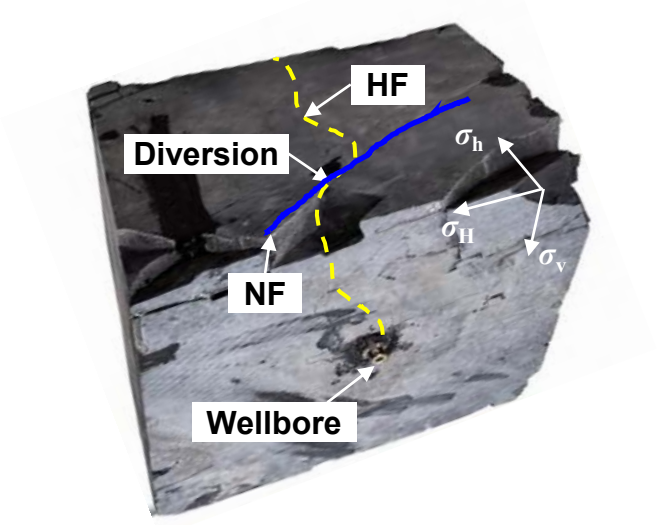

Fracture geometry on the surface

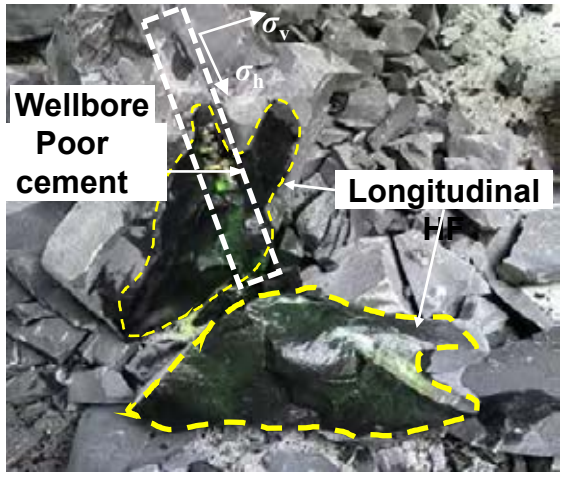

Fracture geometry after splitting the specimen

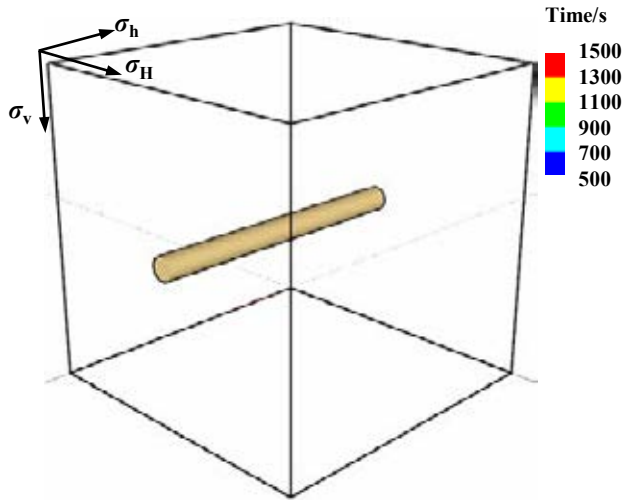

3D-reconstructed dynamic fracture propagation geometries

3. Multi-cluster Propagation Experiment

◆ **Fracturing fluid flows along the cementing interface and forms a longitudinal fracture induced by natural fractures.**

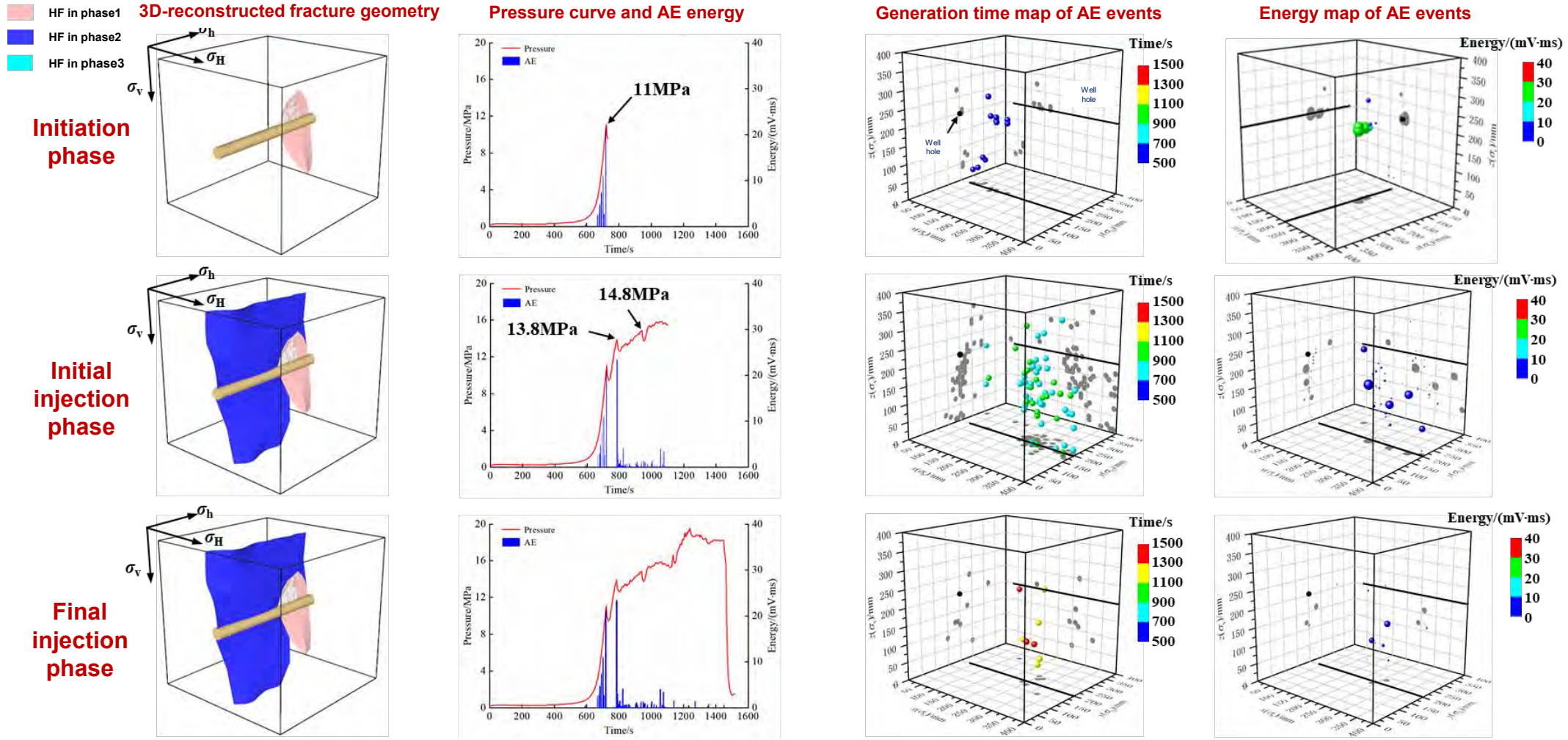

3. Multi-cluster Propagation Experiment

(2) Specimen 2#

Parameter: σ_V=23MPa, σ_H=25MPa, σ_h=20MPa, d_c=21mm, Q=50mL/min

- HF1 is a transverse fracture and it crosses the NF to generate an orthogonal fracture network near the toe of the horizontal wellbore;
- HF2 is also a transverse fracture and it diverts at the NF after initiation to create a step-like propagation geometry;
- HF3 consists of an oblique fracture intersecting the horizontal wellbore and a transverse fracture.

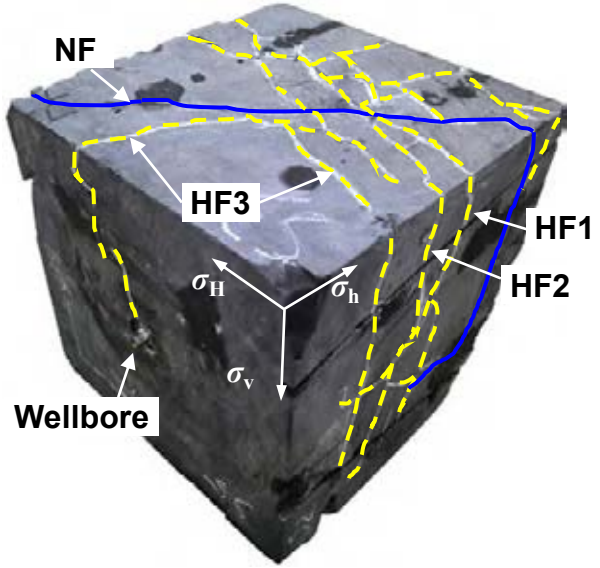

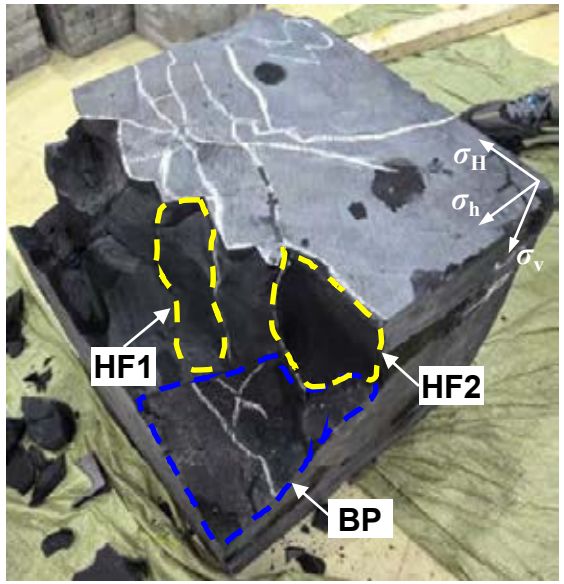

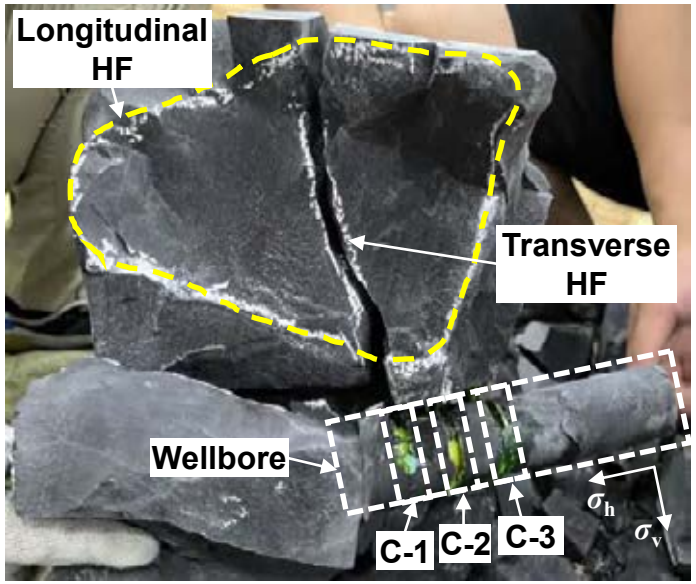

Fracture geometry after splitting the specimen

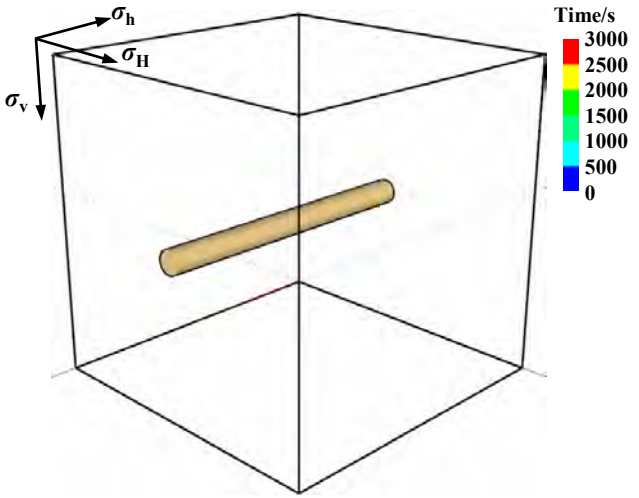

3D-reconstructed dynamic fracture propagation geometries

3. Multi-cluster Propagation Experiment

- During the initiation phase, Cluster 1 forms, generating high-energy AE events at the wellbore axis. In the early stage of injection, the pressure fluctuates violently, Cluster 2 forms a transverse fracture, and Cluster 3 forms a longitudinal fracture.

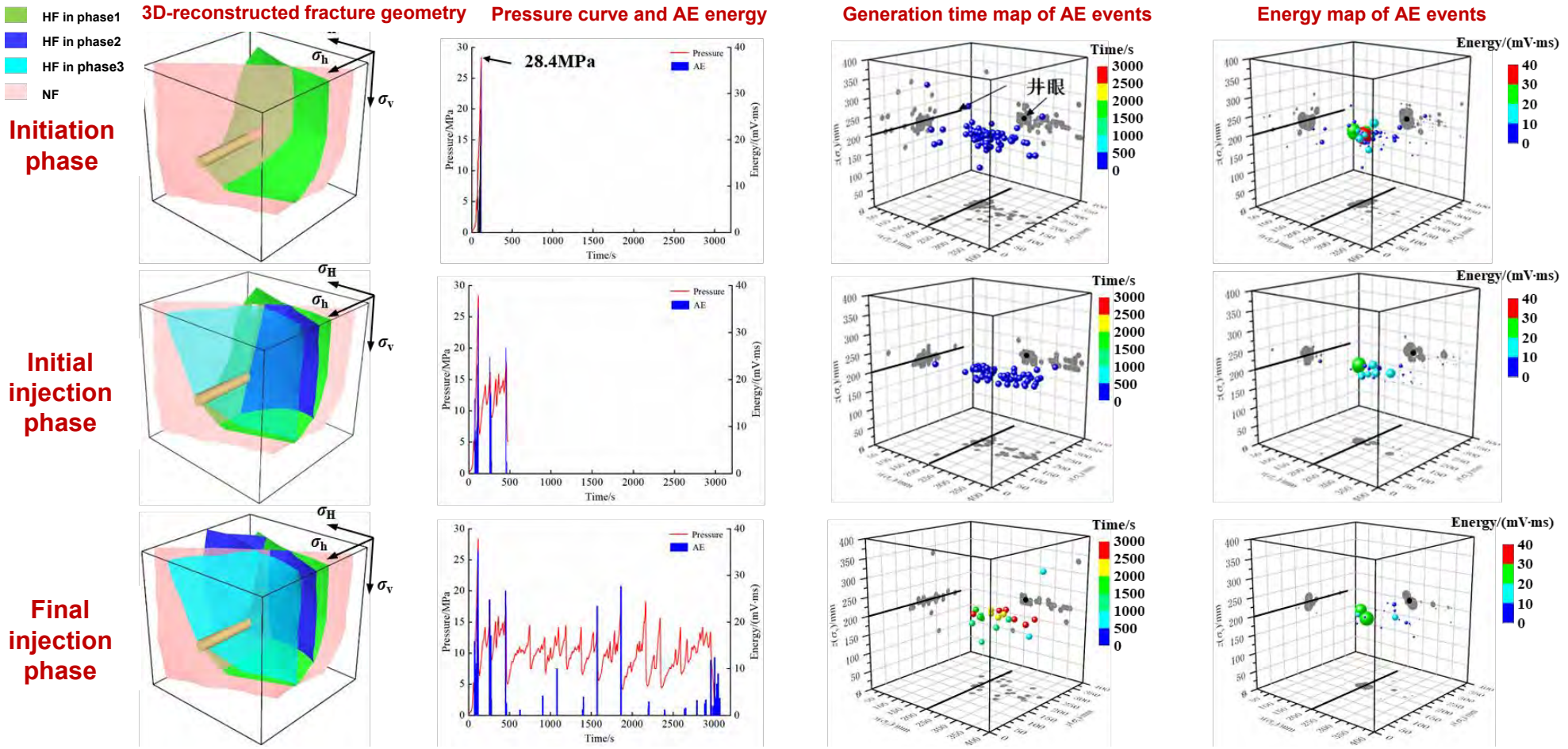

3. Multi-cluster Propagation Experiment

(3) Specimen 5#

Parameter: σ_V=23MPa, σ_H=25MPa, σ_h=20MPa, d_c=11mm, Q=50mL/min

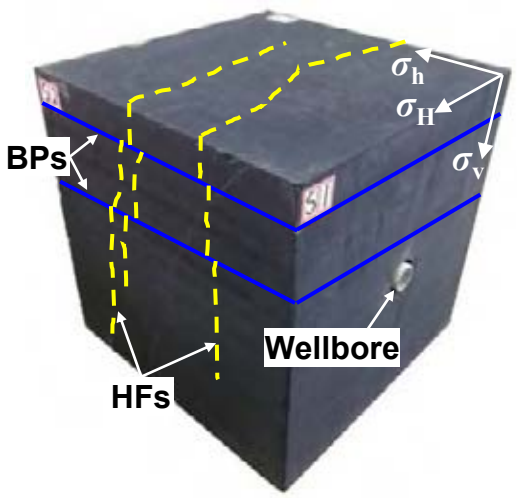

Fracture geometry on the surface

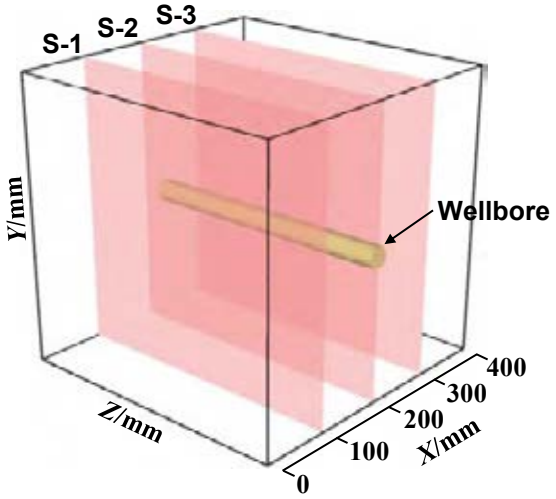

Slicing positions

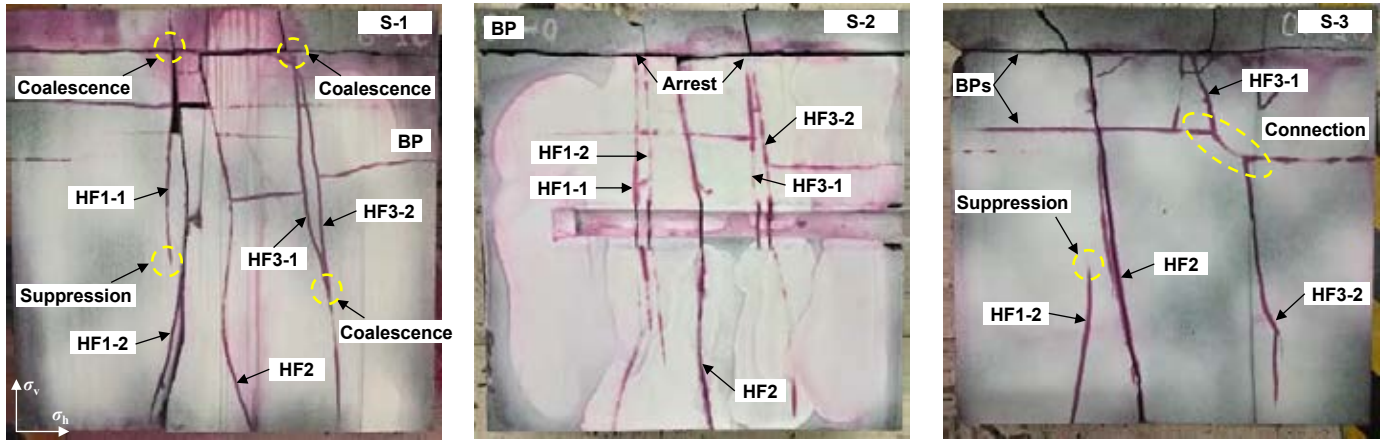

Fracture geometry at different slices

- HF1-1 and HF1-2 are able to propagate in parallel after initiation, as well as HF3-1 and HF3-2;
- HF1-1 and HF1-2 are communicated through the BP as well as HF3-1 and HF3-2;
- The hydraulic energy driving HFs to propagate is gradually consumed as the fracture length increases, causing HFs not to penetrate BPs in the vertical direction and tending to be arrested by BPs. In comparison, multiple clusters of fractures tend to coalesce and form a dominant fracture.

3. Multi-cluster Propagation Experiment

- The simultaneous propagation of multiple clusters of fractures can open and connect multiple BPs. The pressure curve exhibits a multi-peak characteristic, with each pressure drop representing the initiation of a bedding plane fracture, and the rising pressure fluctuation indicates that the injection phase is dominated by the seepage of fracturing fluid along the BPs.

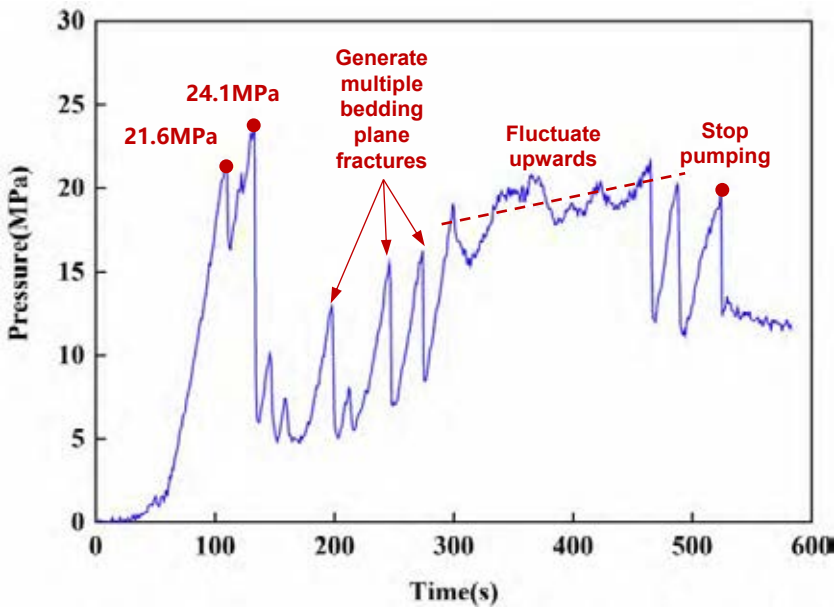

Pressure curve for simultaneous propagation of two clusters in stage 1

Fracture propagation geometries of two clusters in stage 1

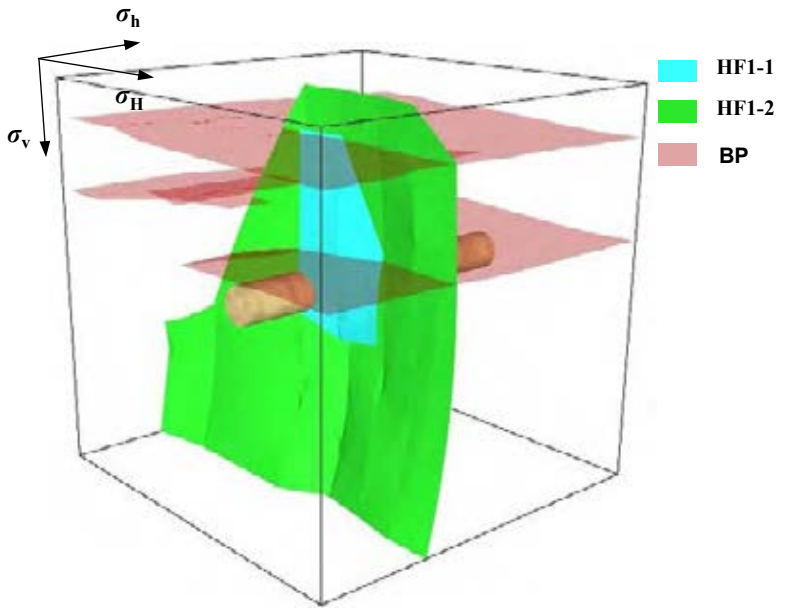

3D-reconstructed fracture propagation geometries of two clusters in stage 1

3. Multi-cluster Propagation Experiment

(4) Specimen 6#

Parameter: σ_V=23MPa, σ_H=25MPa, σ_h=20MPa, d_c=11mm, Q=50mL/min

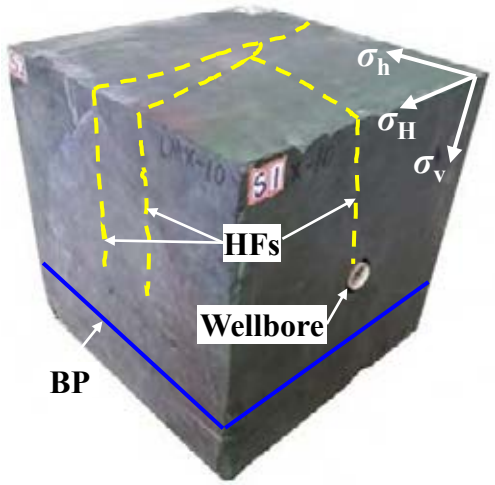

Fracture geometry on the surface

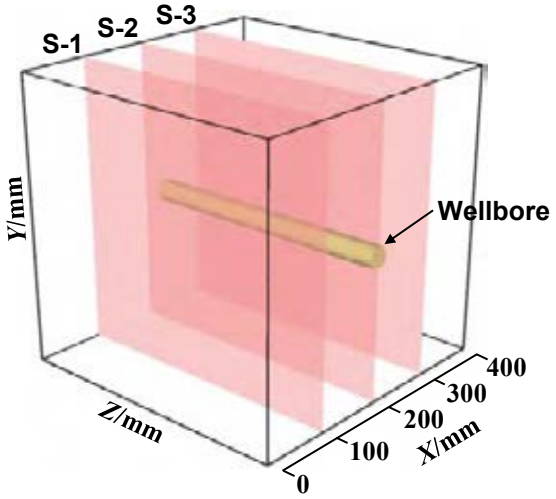

Slicing positions

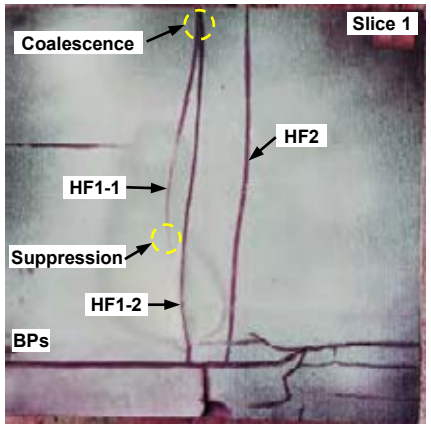

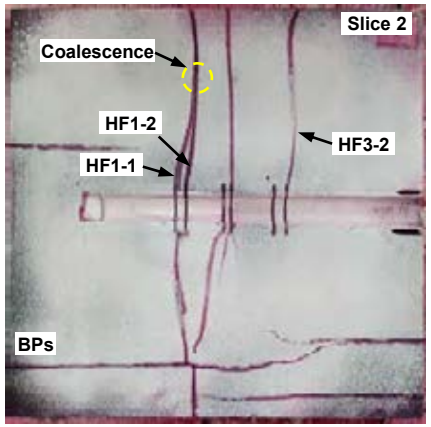

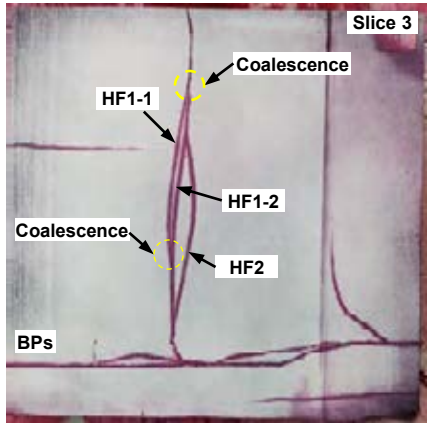

Fracture geometry at different slices

- HF1-1 and HF1-2 can propagate in parallel in the near-wellbore region. In the far-field region, however, their propagation paths in the length and height direction gradually coalesce.
- In stage-1, the lower parts of the perforation clusters initiate one fracture; In stage-2, the upper part of the left perforation cluster does not initiate, while the lower part initiates three HFs; In stage-3, only the upper part of the right perforation cluster initiates, while the left perforation cluster remains intact.

3. Multi-cluster Propagation Experiment

3.3 Experimental results of sequential propagation of multiple fractures

(1) Specimen 3#

Parameter: σ_V=23MPa, σ_H=25MPa, σ_h=20MPa, L_c=33mm, Q=50mL/min

- One approximately transverse HF and one longitudinal HF are created in fracturing stage-1. This transverse fracture intersects the wellbore axis at an angle of about 63°. The longitudinal fracture grows along the wellbore and connects stages-2 and -3, leading to ineffective initiation in these two stages.In this case, the fracturing fluid leaks off along the propagation path of HF1.

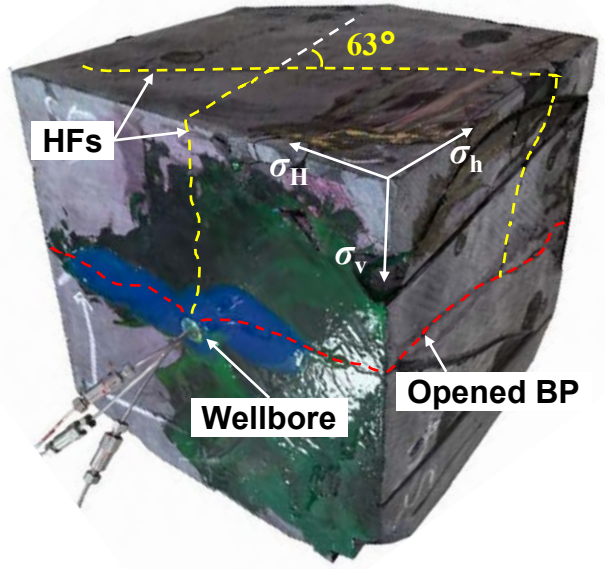

Fracture geometry on the surface

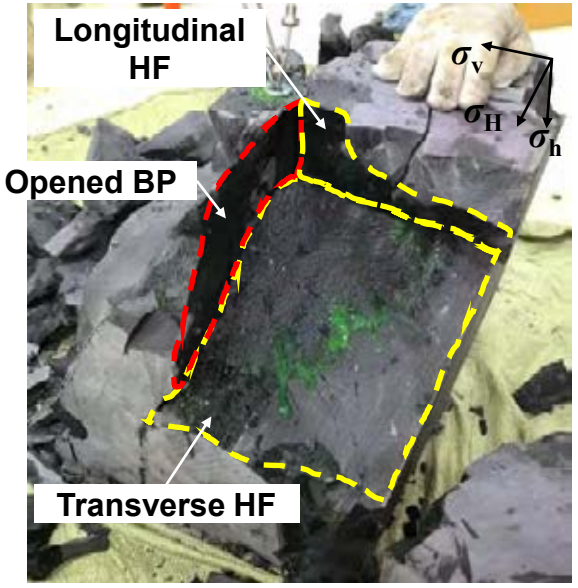

Fracture geometry after splitting the specimen

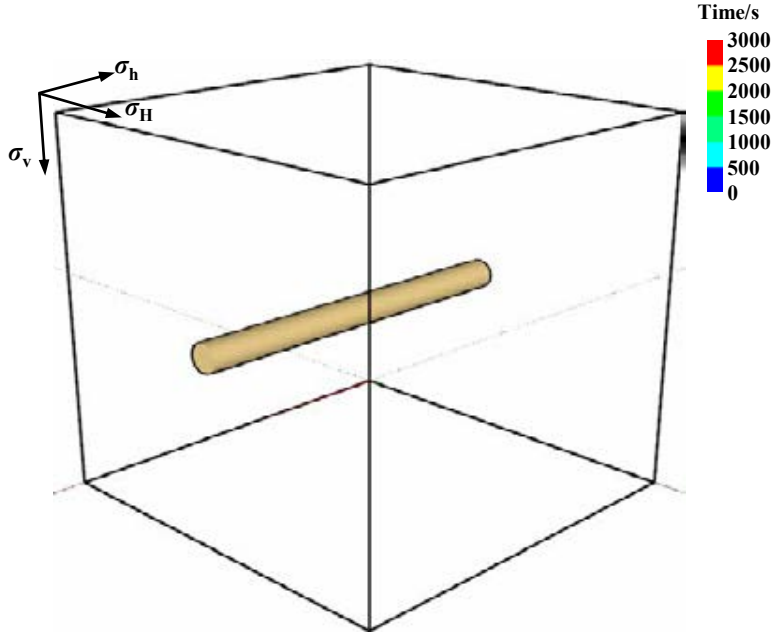

3D-reconstructed dynamic fracture propagation geometries

3. Multi-cluster Propagation Experiment

◆ **The orthogonal geometry of HFs and BPs is formed. After the initiation of stage 1, the pressure fluctuates violently with multiple peaks, and AE events are widely distributed.**

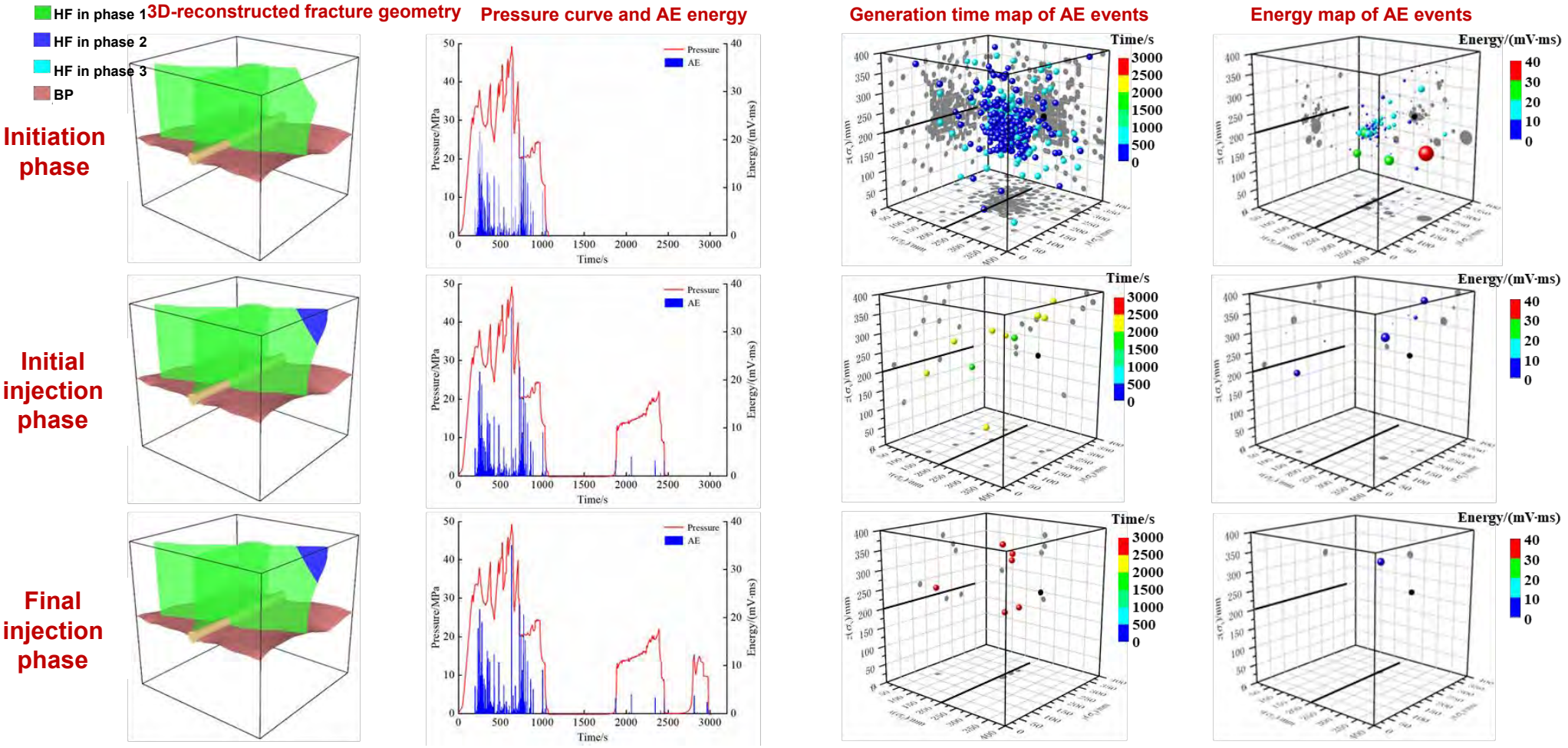

3. Multi-cluster Propagation Experiment

(2) Specimen 4#

Parameter: σ_V=23MPa, σ_H=25MPa, σ_h=20MPa, L_c=33mm, Q=50mL/min

- NF is activated after injection, and the fracturing fluid enters the NF and flows along it, ultimately opening microfractures connecting to the NF and forming an inclined HF communicating with the NF.
- All three fracturing stages initiate to form transverse fractures, but the length and height propagation of those fractures created are suppressed, with fractures mainly distributing in the near-wellbore region.

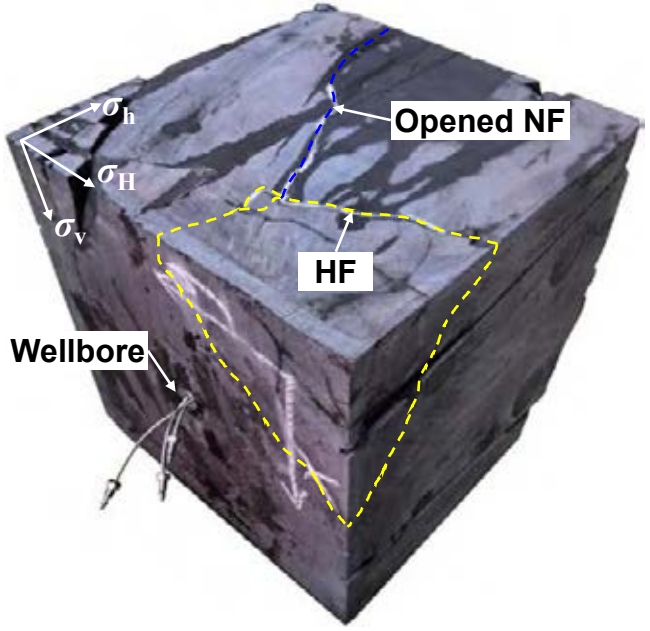

Fracture geometry on the surface

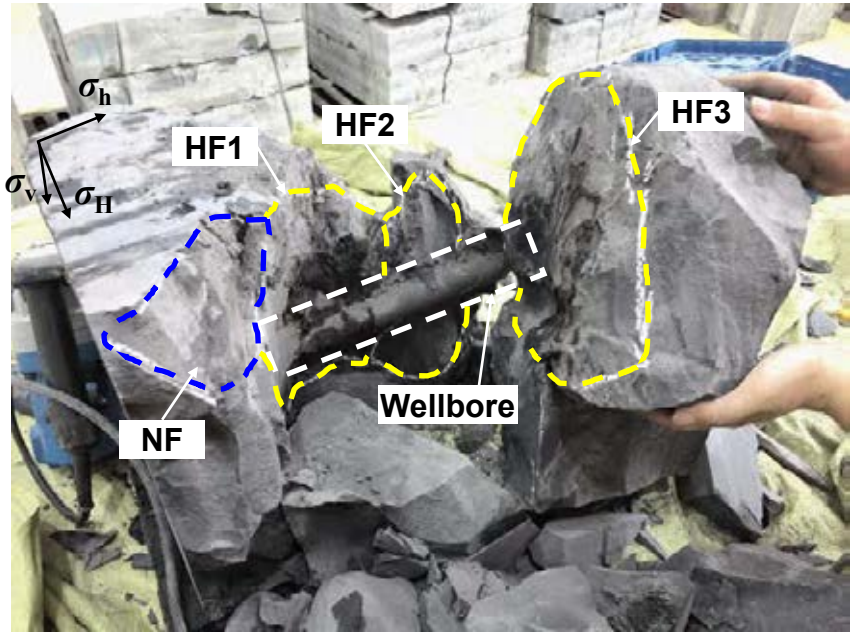

Fracture geometry after splitting the specimen

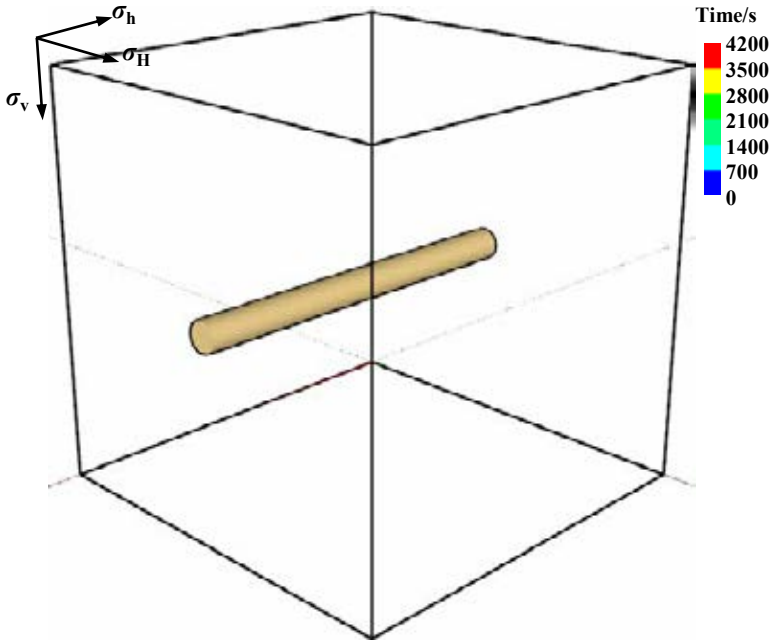

3D-reconstructed dynamic fracture propagation geometries

3. Multi-cluster Propagation Experiment

◆ For The interaction between multi-stage fractures and natural fractures, all three stages of fractures effectively initiated, but the distribution of AE events in the direction of fracture length was restricted.

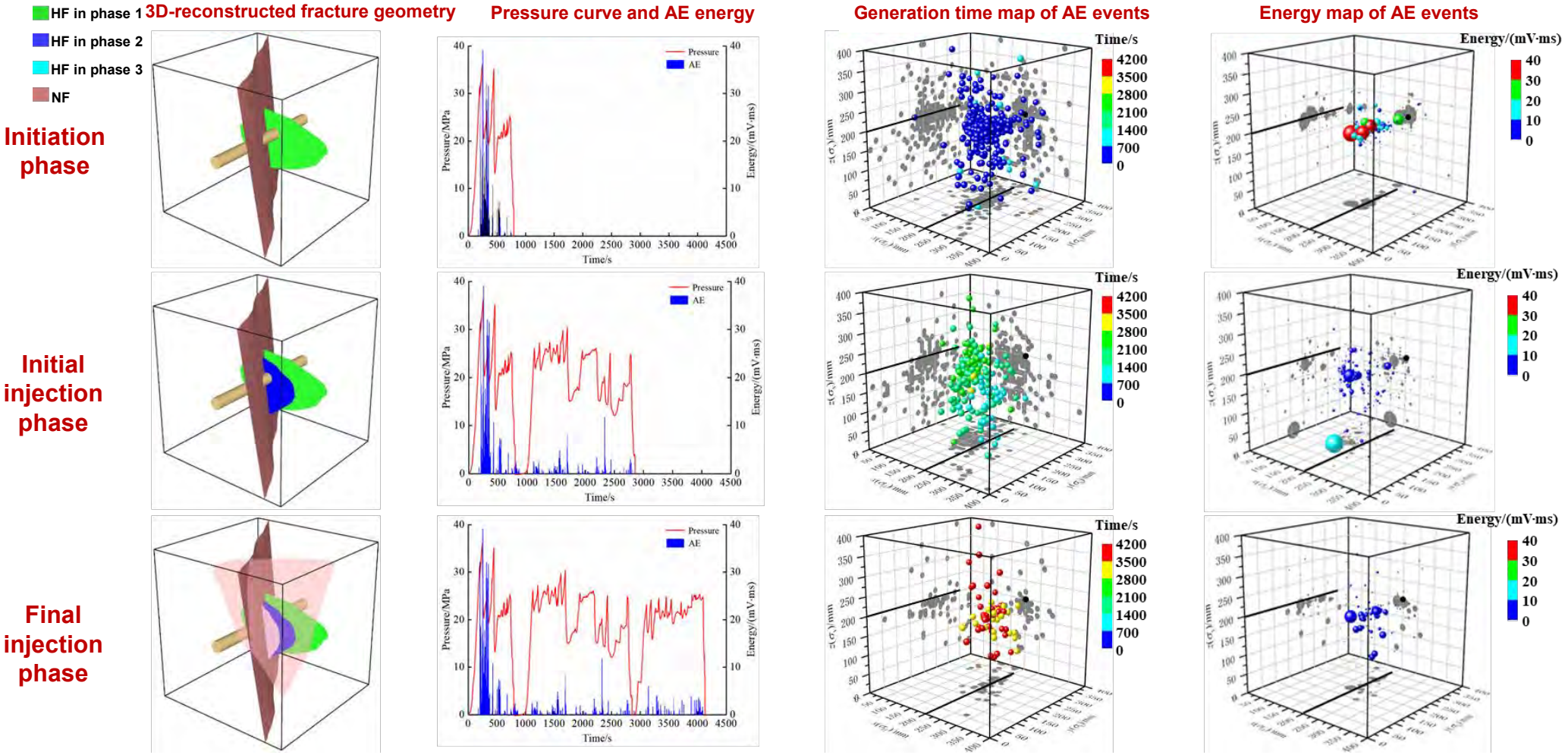

3. Multi-cluster Propagation Experiment

(3) Specimen 5#

Parameter: σ_V=23MPa, σ_H=25MPa, σ_h=20MPa, Q=50mL/min

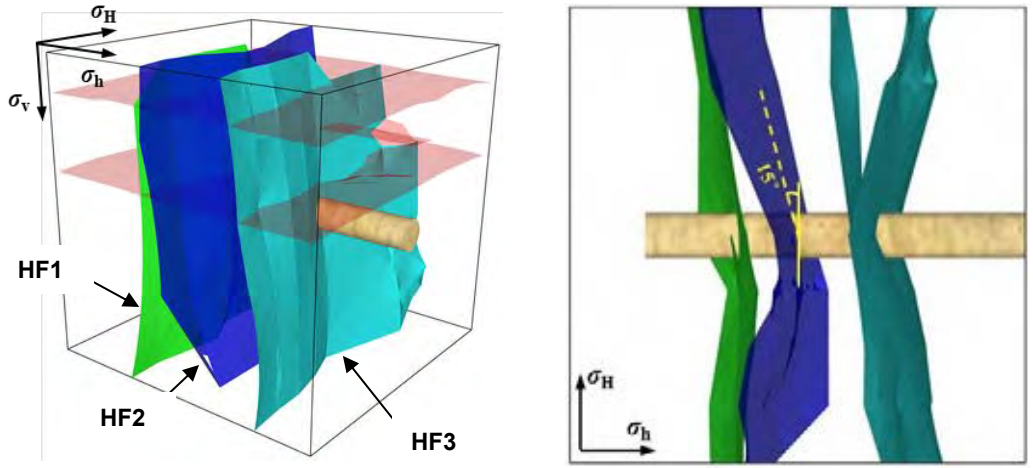

Specimen 5#'s sequential HF propagation geometry (L_s=53mm)

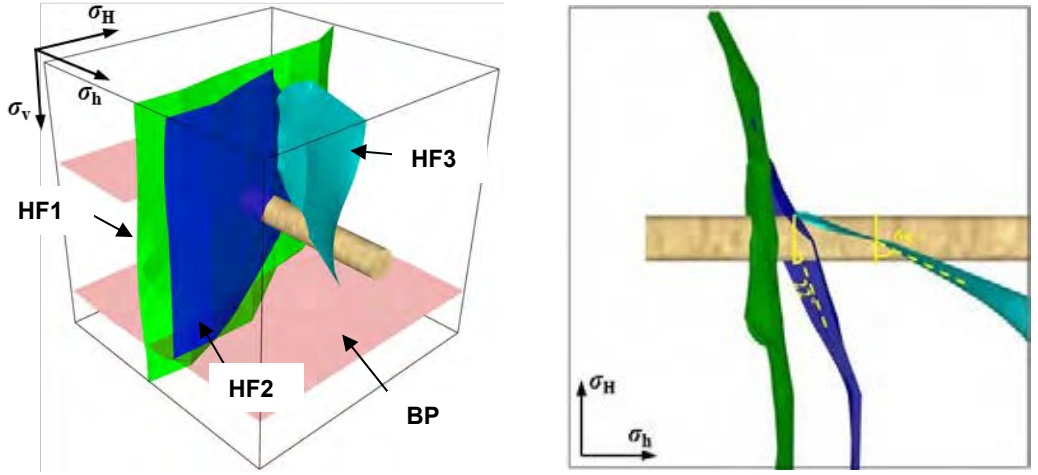

Specimen 6#'s sequential HF propagation geometry (L_s=33mm)

- Under Ls = 53 mm, HF2 deviates toward HF1, with a deflection angle of one wing of 15°. However, HF3 propagates in an approximately planar manner, which is similar to that of HF1.
- Under Ls = 33 mm, HF2 intersects with the horizontal wellbore at a deflection angle of 21°; moreover, HF3 initiates and propagates nearly along the wellbore axis.
- Compared to Ls = 53 mm, the fracture propagation paths under Ls = 33 mm are more significantly affected by stress interference, leading to intersections between subsequent and previously created fractures.

3. Multi-cluster Propagation Experiment

◆ Discussions: Characteristics under different fracture propagation behaviors

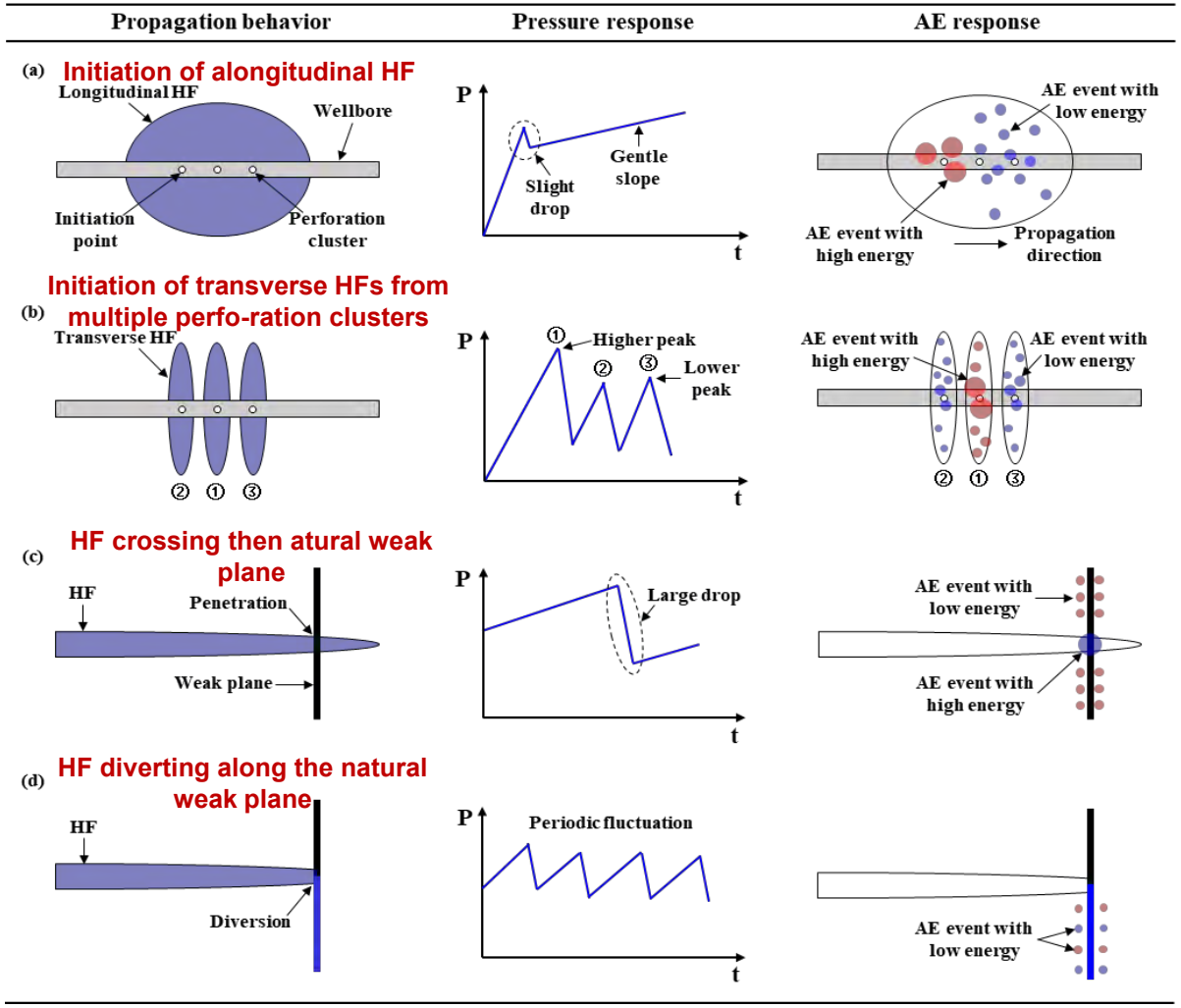

- ◆ **Longitudinal fracture initiation and propagation**: After the breakdown pressure, the pressure initially drops slightly and then rises slowly. High-energy acoustic emission events are concentrated at the initiation point, with numerous low-energy AE events distributed along the wellbore axis.
- ◆ **Non-synchronous initiation of multiple clusters**: The clusters do not initiate simultaneously, with the first peak pressure being relatively high.
- ◆ **Crossing natural fractures**: A significant drop in injection pressure occurs.
- ◆ **Deflection along natural fractures**: Periodic fluctuations in injection pressure occur, with continuous low-energy AE events on the deflection side.

Content

4. Temporary Plugging Fracturing Experiment

- A multi-cluster TPF experimental method based on distributed optical fiber strain monitoring was developed. Experiments on fracture propagation of multi-cluster temporary plugging fracturing in horizontal wells were carried out using a true triaxial experimental system integrating drilling, fracturing and production under high temperature and high pressure.

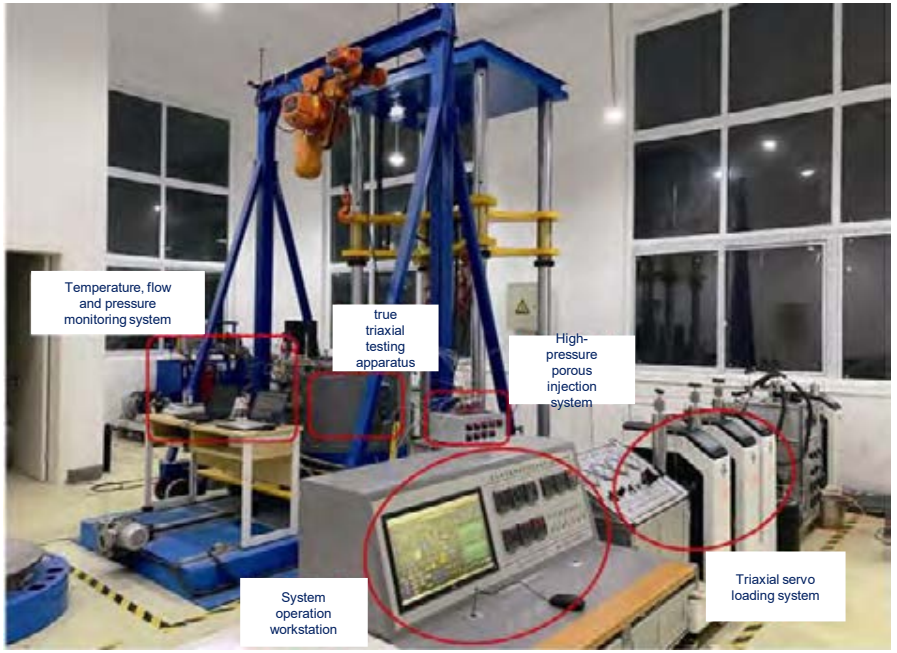

A true triaxial experimental system integrating drilling, fracturing and production

Optical fiber monitoring system

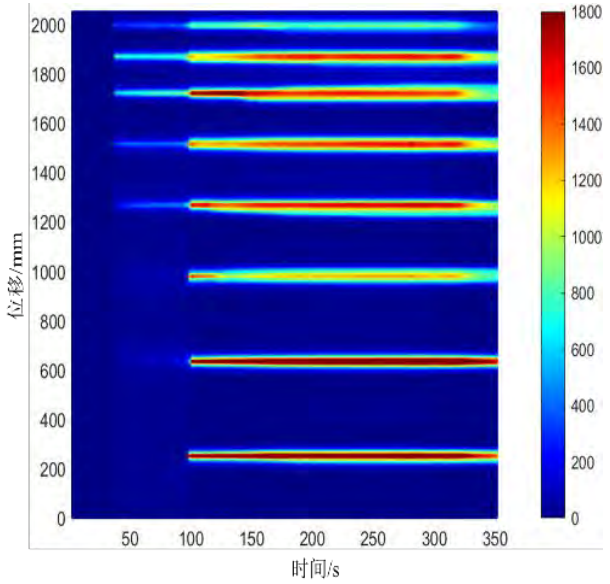

Optical fiber response to multi-cluster fracture propagation

4. Temporary Plugging Fracturing Experiment

4.1 Experimental scheme

(1) Distributed optical fiber pre-processing

- **Optical Fiber Splicing:** Use a optical fiber cutter to make the end face flat. After optical fiber splicing, use a heat shrink tube to provide protection for the spliced area.
- **Calibration of Measurement Section:** Apply stress to the starting point and end point of the U-shaped optical fiber respectively. Take the midpoint of the section that generates strain as the starting distance and ending distance of the measurement section.

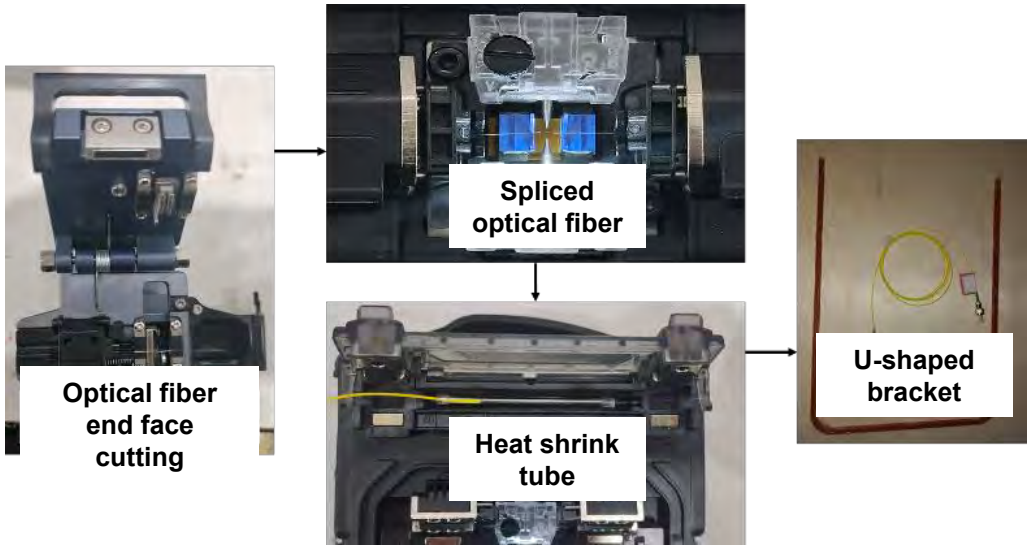

Optical fiber preparation

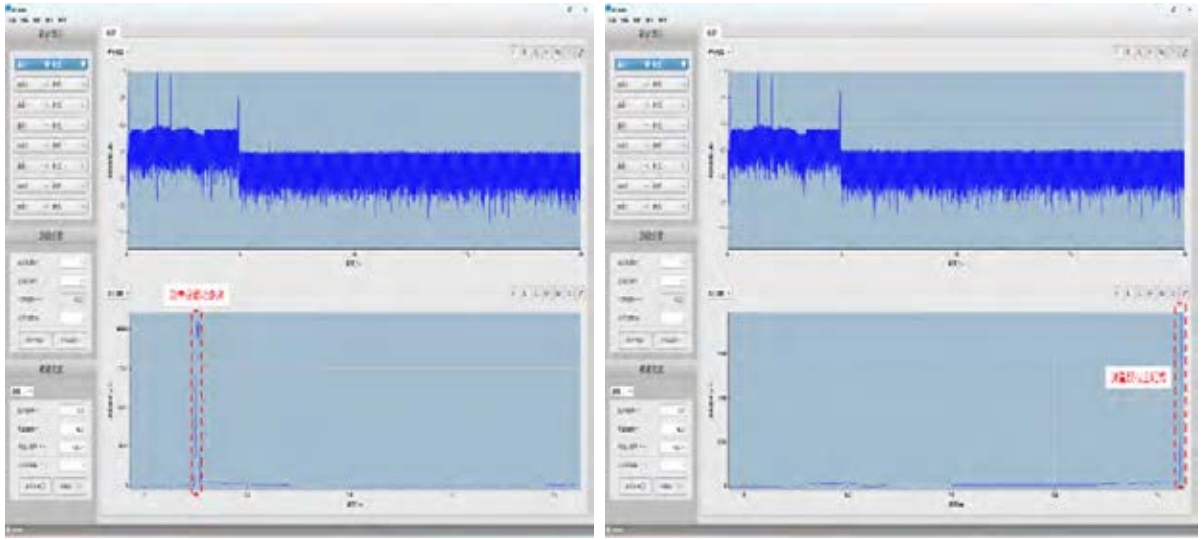

Calibration of the optical fiber measurement section

4. Temporary Plugging Fracturing Experiment

(2) Specimen preparation

- **Wellbore Fabrication:** After inserting the wellbore vertically into the cement mortar, ensure that the height of the middle perforation cluster is **200 mm**.
- **Optical fiber Placement:** First, lay a **10 cm** thick layer of cement mortar in a $400^3 mm^3$ mold. Then, place the U-shaped optical fiber bracket and the wellbore vertically in the mortar. Lay **three U-shaped optical fiber (marked as 1#–3#)** evenly in a direction parallel to the wellbore.

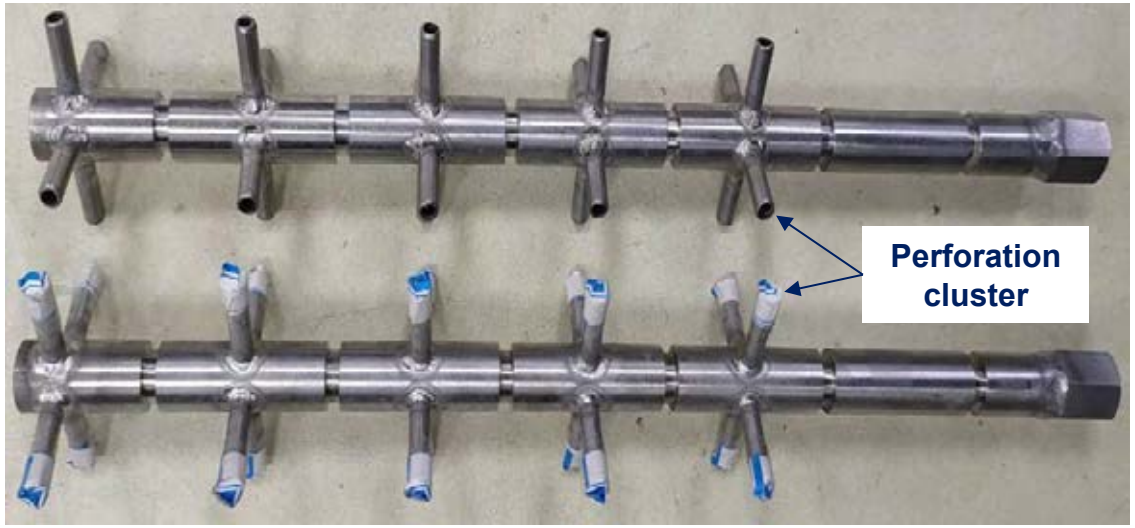

Wellbore with welded simulated perforation clusters

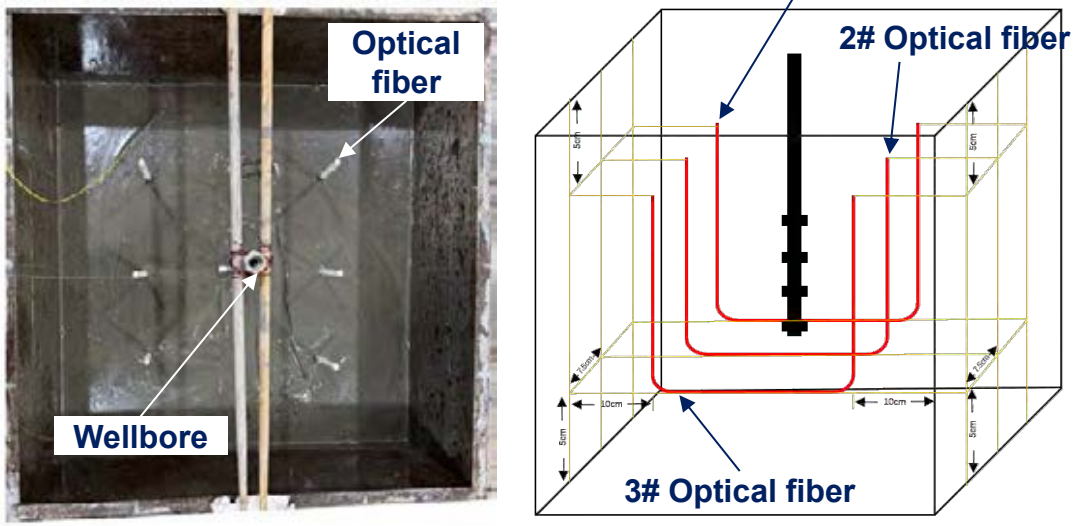

Rock sample casting and optical fiber placement scheme

4. Temporary Plugging Fracturing Experiment

(3) Parameter design

◆ Taking into account the equipment performance and similarity criteria, the parameters are set as follows: σ_V=30MPa、σ_{Hmax}=22~28MPa、σ_{hmin}=10MPa，Considering the field fracturing construction rates of 12–18 m³/min and the fracturing fluid viscosity of 5–10 mPa·s, the laboratory injection rates are calculated to be 20–50 mL/min.

- Scaling of the propagation regime:

$$\mu_1 = \mu_f \left[\frac{t_{\max,1}}{t_{\max,f}} \left(\frac{Q_f}{Q_1} \right)^{3/2} \left(\frac{E_f}{E_1} \right)^{13/2} \left(\frac{K_1}{K_f} \right)^{9} \right]^{2/5}$$

$$t_{\max} = \frac{R_{\max}^{5/2} K}{QE}$$

- Geometrical scaling

$$\frac{S_1}{S_f} = \frac{L_1}{L_f}$$

Parameter design scheme

No	Temporary plugging (TP) agent size	Injection rate for TP/mL/min	Horizontal stress difference/MPa	Number of clusters	Cluster spacing/cm
1	70-140	30	15	3	3
2	6mm fiber				5
3	160-200				7
4	6mm fiber	50	15	4	5
5		30			
6		20			
7	70-140	30	12	5	5
8			15		
9			18		

4. Temporary Plugging Fracturing Experiment

(4) Feasibility verification of optical fiber support

- Design a spiral-shaped optical fiber support structure to verify whether the material of the support will induce the formation of weak planes, test the matching degree between the fracture morphology obtained from the optical fiber monitoring and actuality.
- The maximum radius of the helix R=150mm, the pitch p=30mm, and design a circular base with a reserved diameter d=30mm. Design a built-in support structure to ensure that each helical layer remains coplanar during the pouring process.

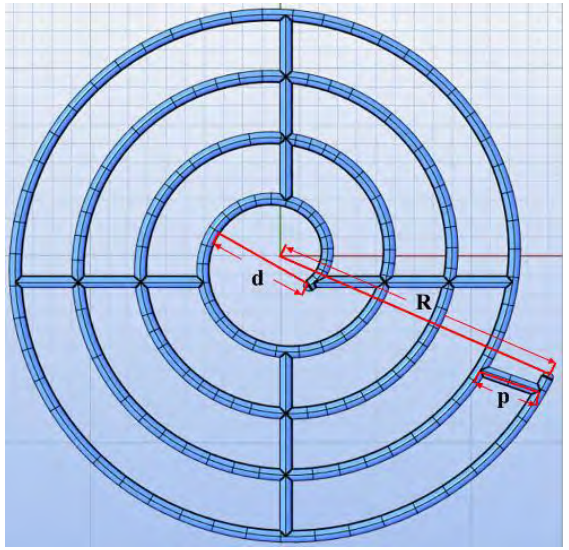

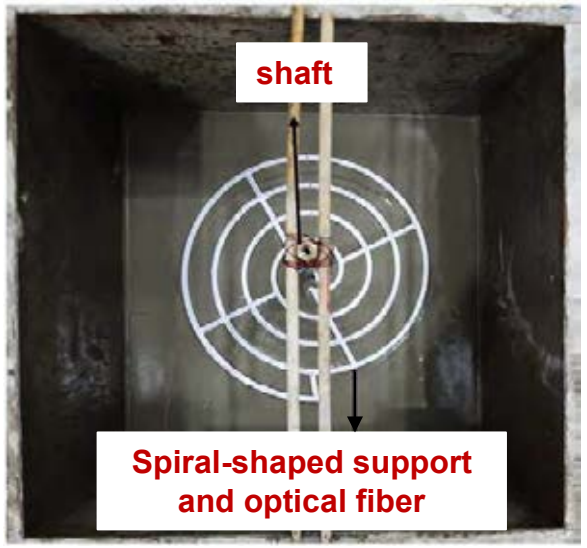

Spiral-shaped optical fiber support and laying scheme

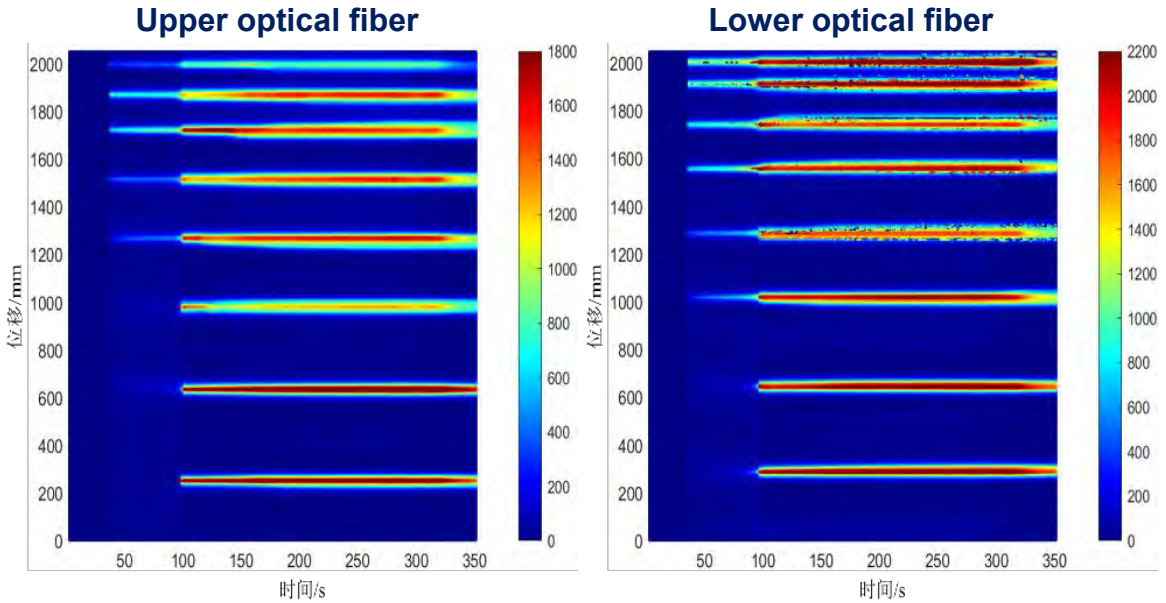

Fiber optic monitoring results

4. Temporary Plugging Fracturing Experiment

- The fracture pressure of the specimen was **10.18 MPa**. After the pressure application, a **vertical fracture** was formed. This fracture could pass through each spiral layer of the optical fiber support in sequence, The fracture did not deviate along the support structure.
- The position of the optical fiber strain response is **highly consistent** with the intersection point of the fracturing fracture and the optical fiber support.

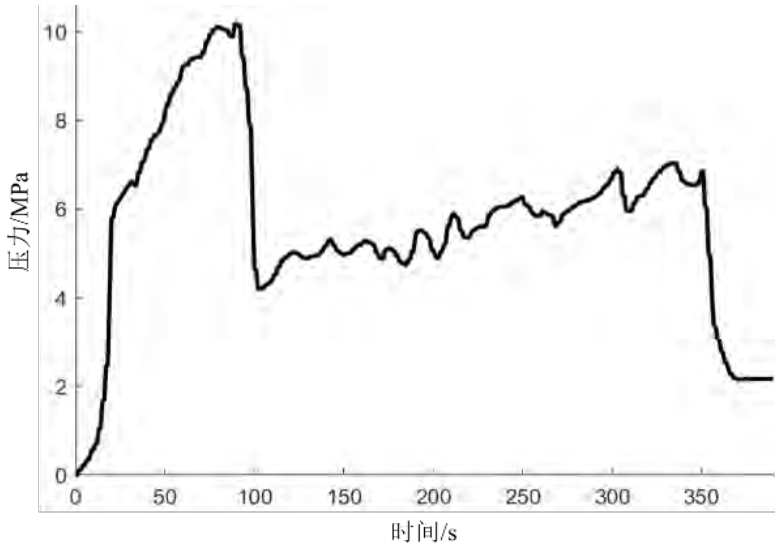

HF pumping pressure curve

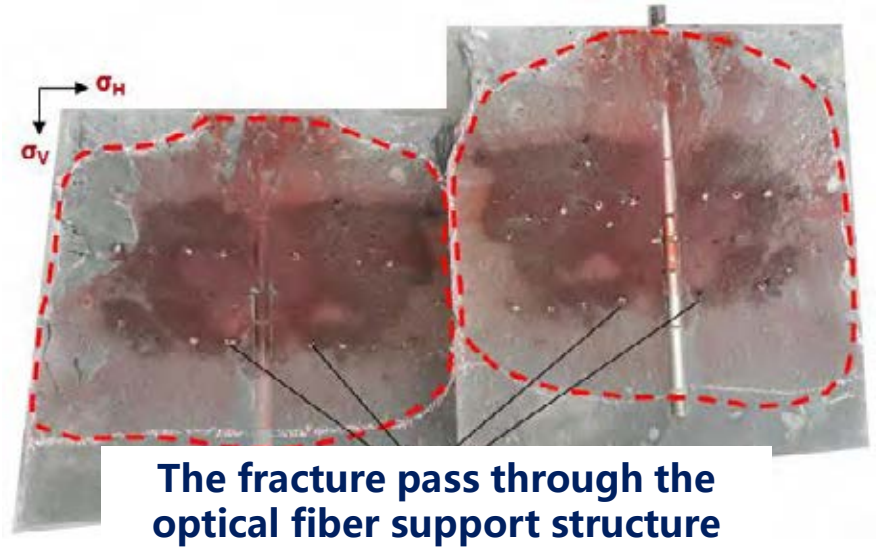

The fracture pass through the optical fiber support structure

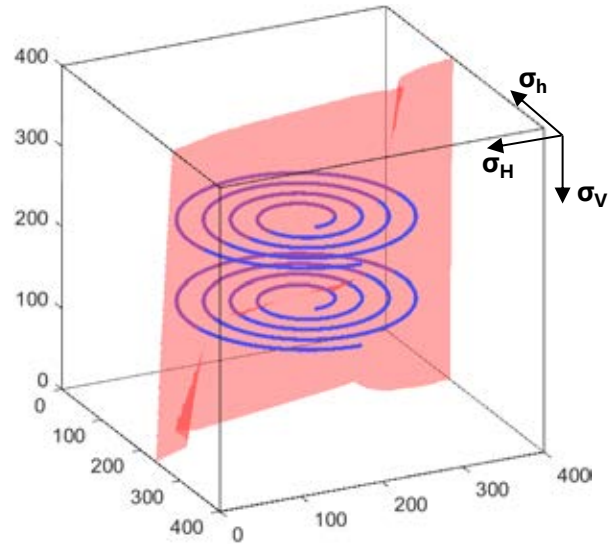

The morphology of the fracture obtained based on the fiber optic monitoring data

Parameter: σ_V=25MPa, σ_H=20MPa, σ_h=15MPa, Q=30mL/min

4. Temporary Plugging Fracturing Experiment

4.2 HF geometry and fiber response under different cluster spacings

(1) Specimen 1#

Parameters: Q=30mL/min, 3 clusters, d_c=3cm, $\Delta\sigma$=15MPa, 70/140 TP particle

- The initial fracturing pressure was **11.63 MPa**, while the fracturing pressure during the TPF was **21.22 MPa**, with an increase of 82.46%.
- The initial fracturing of the three clusters of perforations all resulted in the formation of transverse fractures. The fractures in the cluster 1 could fully expand, while the other clusters did not expand sufficiently. After the TPF, the fractures in the third cluster further expanded.

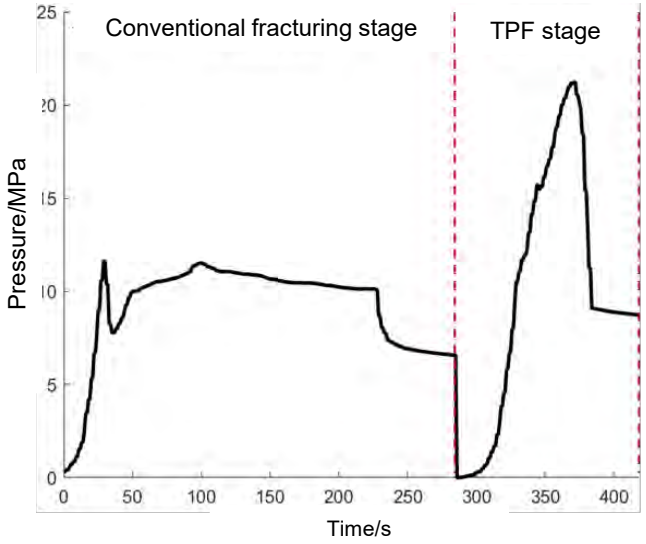

Specimen 1#'s full-process pumping pressure curve

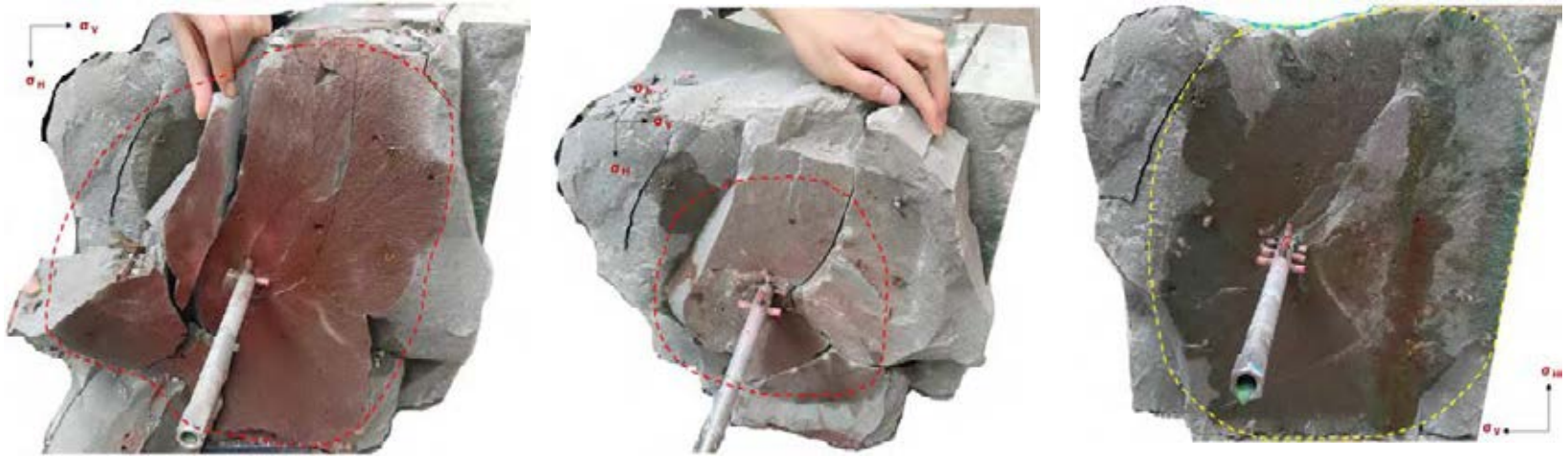

(a) The first cluster of fracture (b) The second cluster of fracture (c) The third cluster of fracture

Specimen 1#'s hydrological fracture morphology

4. Temporary Plugging Fracturing Experiment

- Under a 3cm cluster spacing, the initial fracturing resulted in two symmetrical strain bands. The central area had a lower strain.
- During the TPF stage, clusters 1 and 2 were successfully sealed, and the fractures of cluster 3 were further expanded. Due to the small gap between the fractures, the strain bands of different clusters intersected.

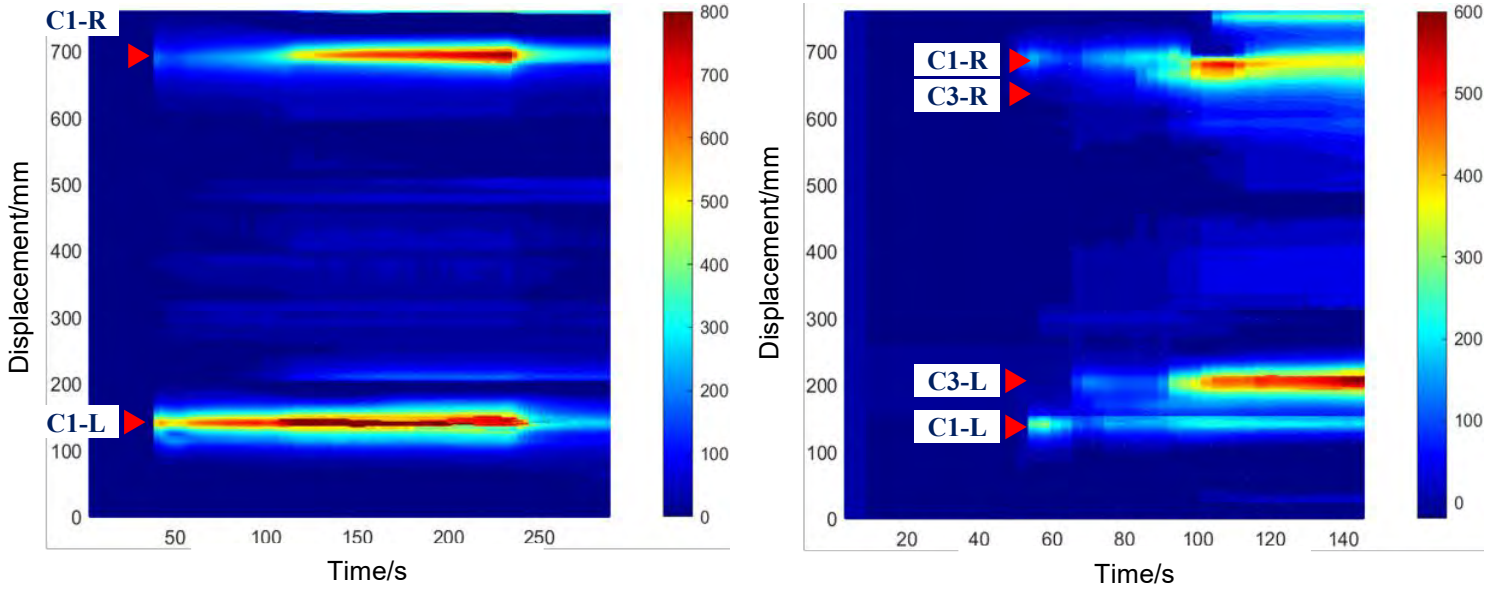

(a) before TPF (b) after TPF

Before and after the TPF of specimen 1, the 1# optical fiber waterfall diagram

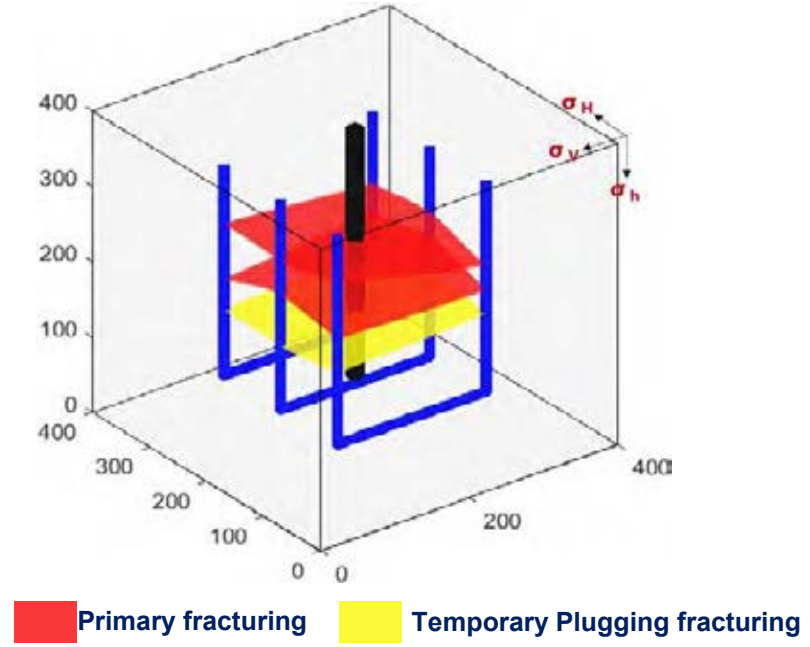

Reconstruction of fracture displacement

Parameters: Q=30mL/min, 3 clusters, d_c=3cm, $\Delta\sigma$=15MPa, 70/140 TP particle

4. Temporary Plugging Fracturing Experiment

(2) Specimen 2#

Parameters: Q=30mL/min, 3 clusters, d_c=5cm, $\Delta\sigma$=15MPa, 6mm TP fiber

- The initial fracturing pressure was **14.61 MPa**, while the fracture fracturing during the TPF stage was **25.81 MPa**, with an increase rate of 76.66%.
- The initial fracturing of the three clusters of perforations all resulted in the formation of transverse fractures. However, only the fractures in cluster 1 could fully expand, After the TPF, the fractures in clusters 2 and 3 further extended to the surface of the specimen.

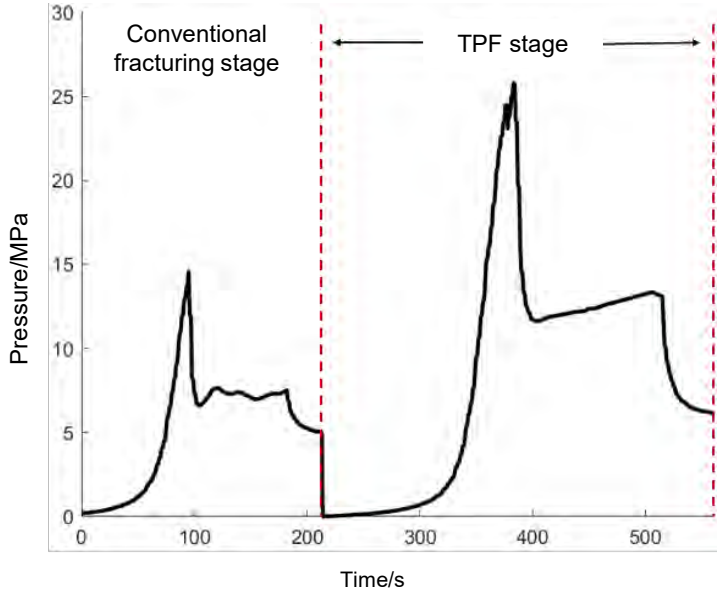

Specimen 2#'s full-process pumping pressure curve

(a) The first cluster of fracture (b) The second cluster of fracture (c) The third cluster of fracture

Specimen 2#'s hydrological fracture morphology

4. Temporary Plugging Fracturing Experiment

- Under a cluster spacing of 5 cm, the initial fracturing created two symmetrical strain bands. The middle area had a smaller strain, indicating that cluster 1 had fully fractured and formed symmetrical fractures.
- During the stage of TPF, the sealing of cluster 1 was achieved. Further, the fractures of the other were expanded. Due to the increase in cluster spacing, the interference effect of inter-fiber stress decreased.

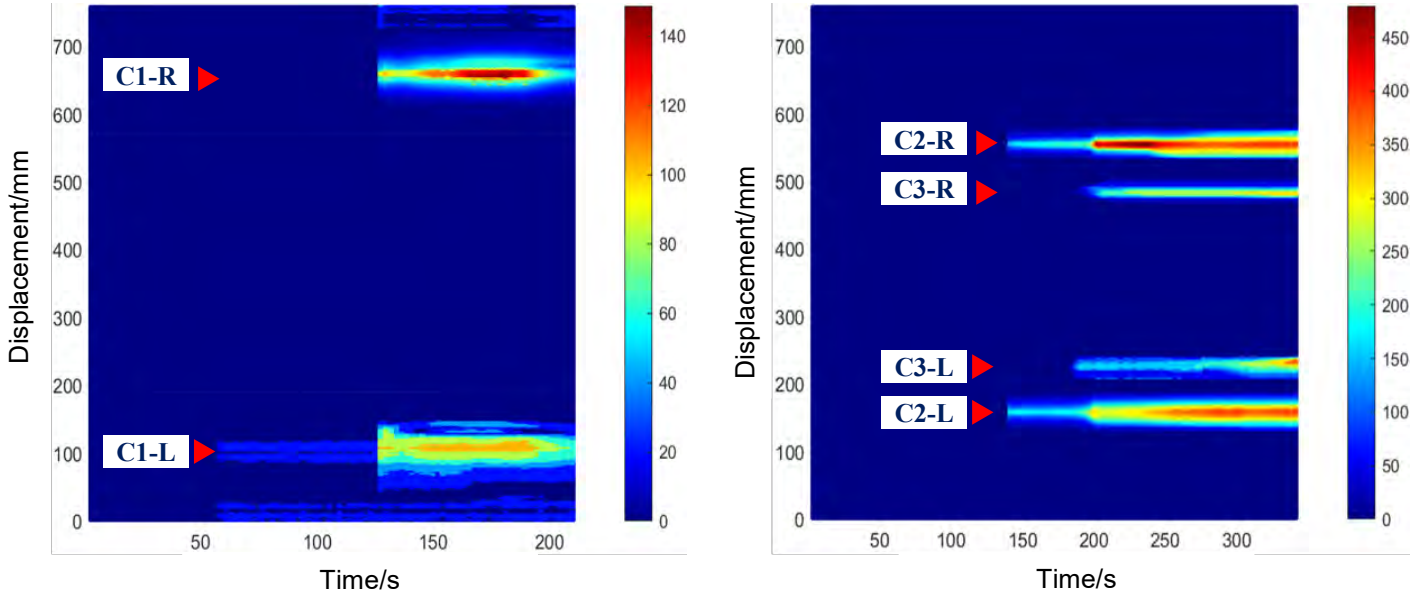

(a) before TPF (b) after TPF

Before and after the TPF of specimen 2, the 2# optical fiber waterfall diagram

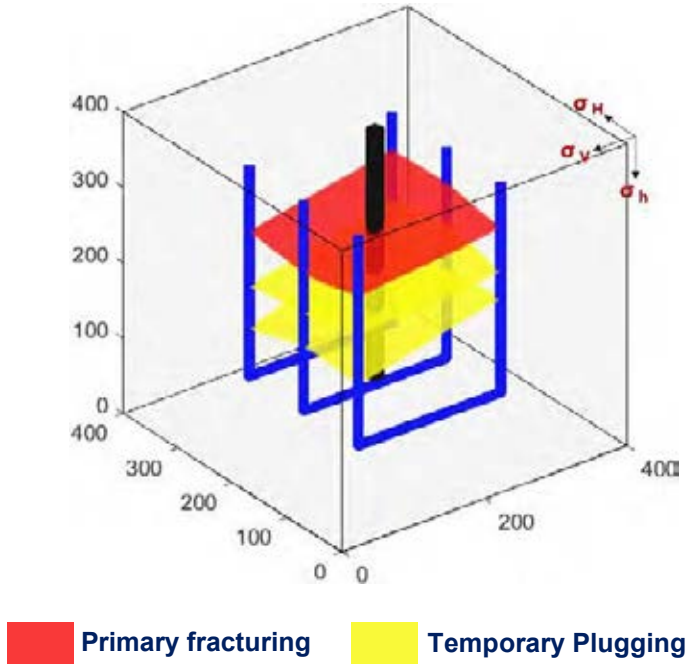

Reconstruction of fracture displacement

Parameters: Q=30mL/min, 3 clusters, d_c=5cm, $\Delta\sigma$=15MPa, 6mm TP fiber

4. Temporary Plugging Fracturing Experiment

(3) Specimen 3#

Parameters: Q=30mL/min, 3 clusters, d_c=7cm, $\Delta\sigma$=15MPa, 160/200 TP particle

- The initial fracturing pressure was **12.54 MPa**, while the fracture fracturing during the TPF was **20.25 MPa**, with an increase of 61.48 %.
- The initial fracturing of the three clusters resulted in relatively low fluid injection volumes. Only cluster 1 expanded to a small area, while clusters 2 and 3 did not effectively fracture. After the TPF, all three clusters' fractures extended to the surface of the specimen.

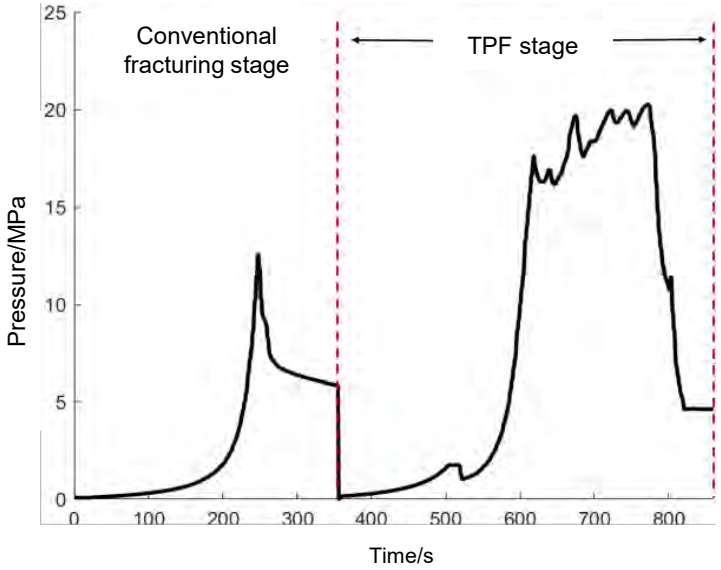

Specimen 3#'s full-process pumping pressure curve

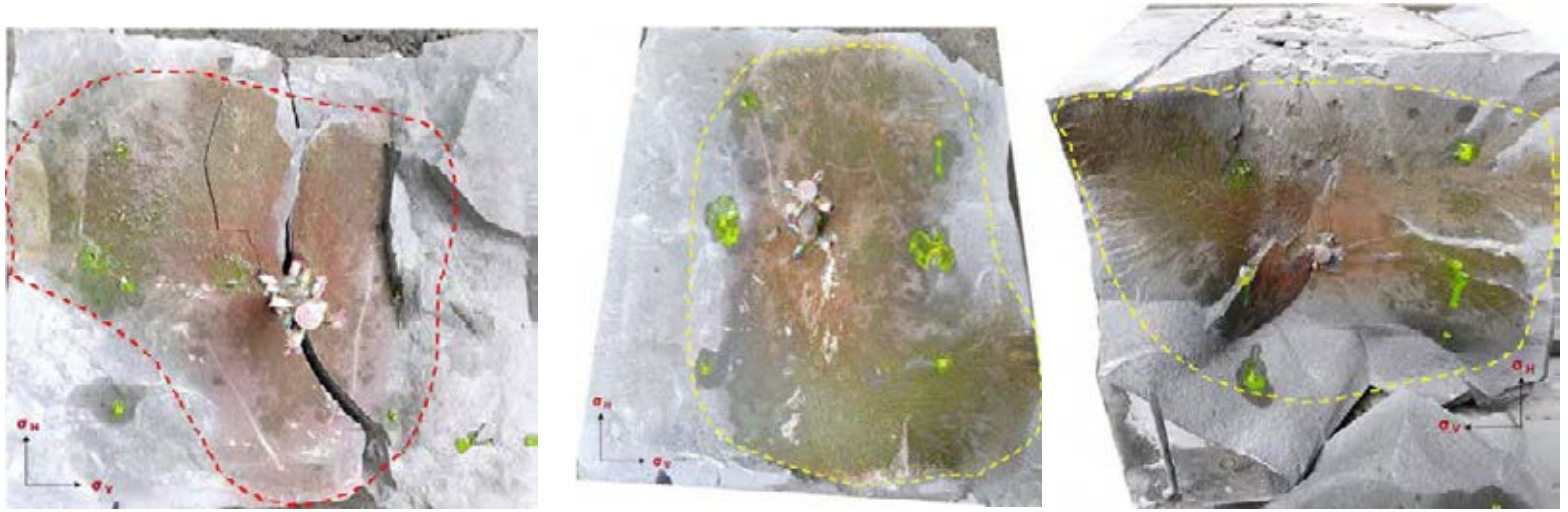

(a) The first cluster of fracture (b) The second cluster of fracture (c) The third cluster of fracture

Specimen 3#'s hydrological fracture morphology

4. Temporary Plugging Fracturing Experiment

- Under a cluster spacing of 7 cm, the initial fracturing resulted in two symmetrical strain bands. The central area had a lower strain, indicating cluster 1 had fully fractured and formed symmetrical fractures.
- During the TPF, clusters 2 and 3 were opened. The strain bands generated on the optical fiber waterfall diagram were wider than those of the previous two samples, indicating that the stress shadow effect between the fractures has decreased and the fracture morphology has become more straight.

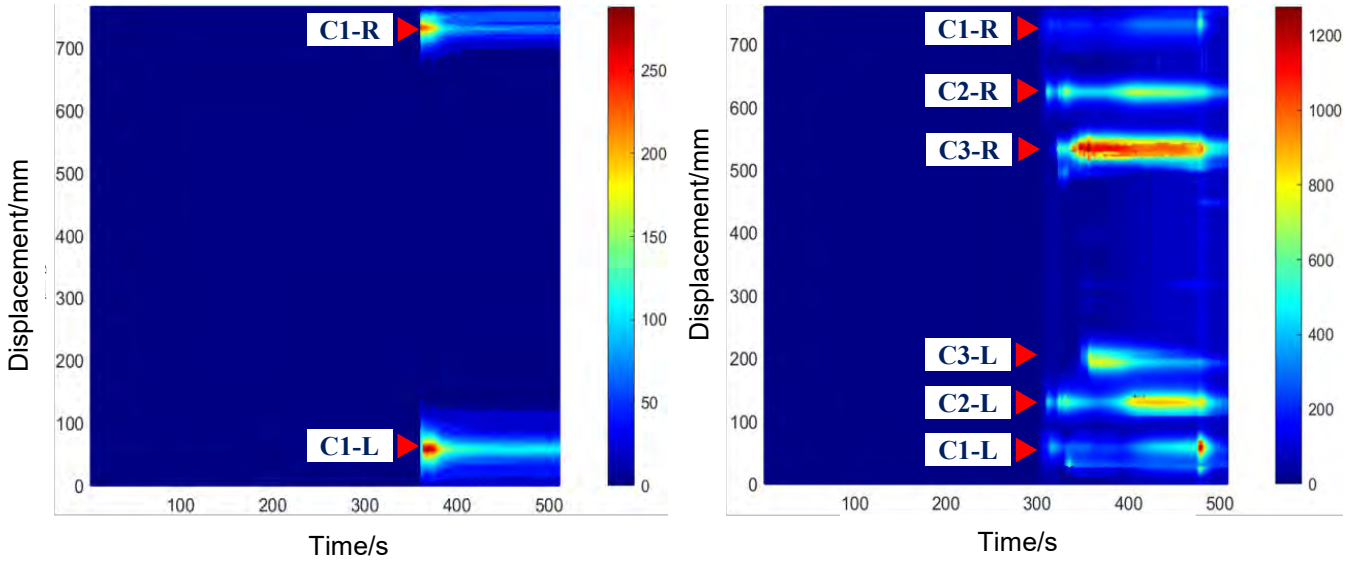

(a) before TPF (b) after TPF

Before and after the TPF of specimen 3, the 3# optical fiber waterfall diagram

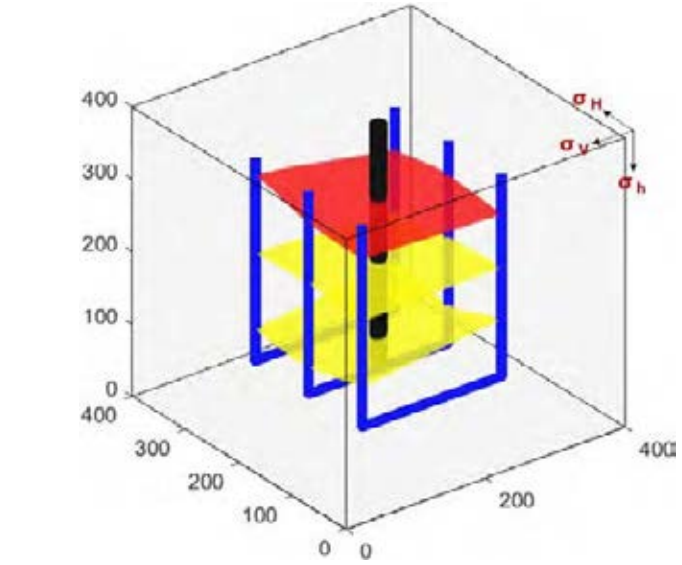

Reconstruction of fracture displacement

Parameters: Q=30mL/min, 3 clusters, d_c=7cm, $\Delta\sigma$=15MPa, 160/200 TP particle

4. Temporary Plugging Fracturing Experiment

(4) Discussion

- The **small cluster spacing** will intensify **the stress shadow effect** between adjacent fractures, hindering the expansion of the central fractures. **The large cluster spacing can weaken the stress interference**, allowing the fractures to approach a more balanced expansion mode.

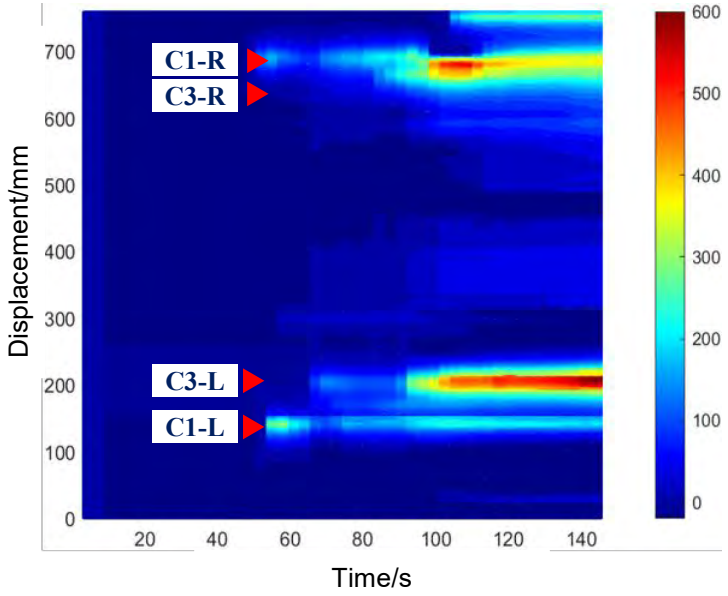

Cluster spacing: 3 cm

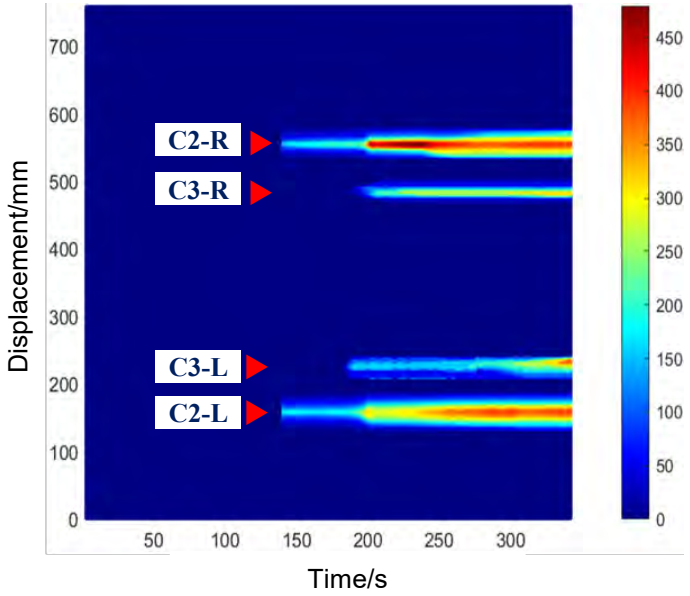

Cluster spacing: 5 cm

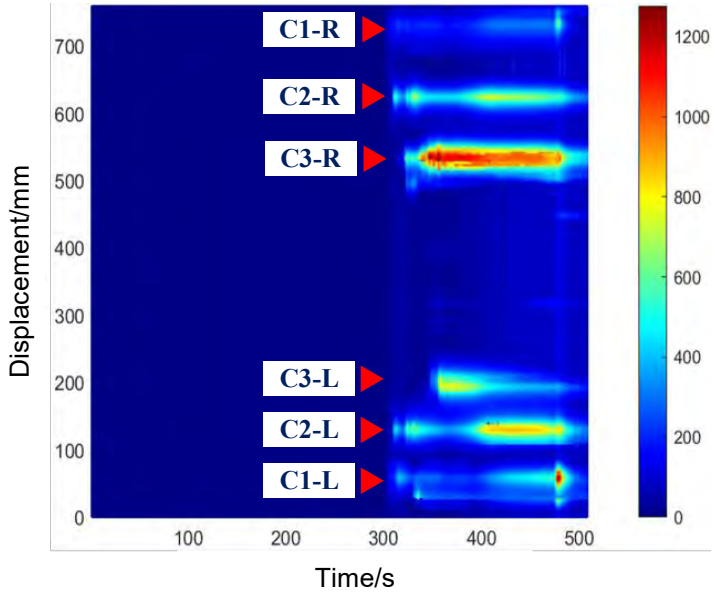

Cluster spacing: 7 cm

The fracture extensions of TPF

4. Temporary Plugging Fracturing Experiment

4.3 HF geometry and fiber response under different pumping rates

(1) Specimen 4#

Parameters: Q=50mL/min, 4 clusters, d_c=5cm, $\Delta\sigma$=15MPa, 6mm TP fiber

- The initial fracturing pressure was 8.59 MPa, while the fracture fracturing during the TPF was 45.7 MPa, with an increase of 432.01 %.
- The initial fracturing only initiated fracture cluster 1, while the TPF initiated fracture cluster 4. Additionally, a longitudinal fracture connecting cluster 1 to cluster 4 and parallel to the wellbore direction was also formed. The final fracture pattern presented a "H" shape.

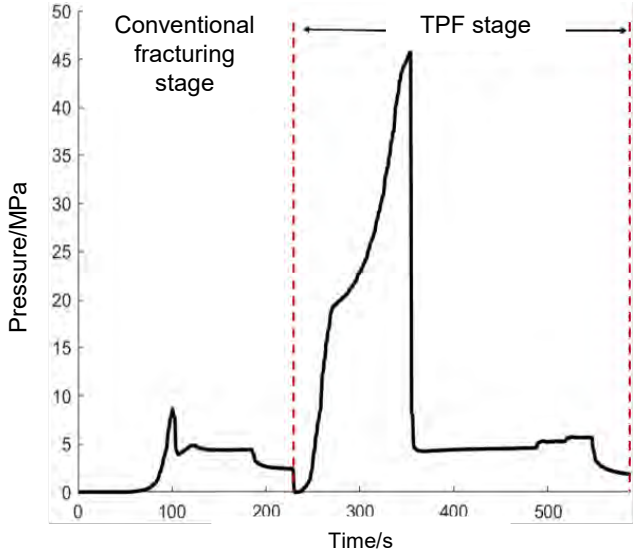

Specimen 4#'s full-process pumping pressure curve

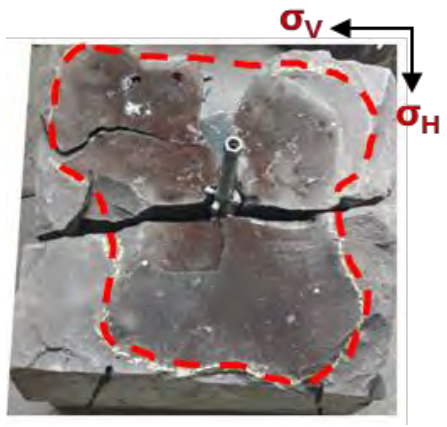

(a) The first cluster of fracture

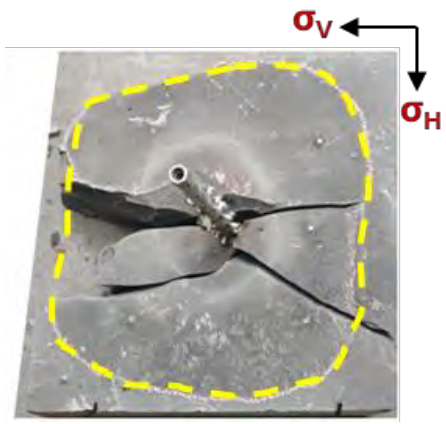

(b) The fourth cluster of fracture

(c) The longitudinal fracture between the first to fourth clusters

Specimen 4#'s hydrological fracture morphology

4. Temporary Plugging Fracturing Experiment

- Under a pumping rate of 50 mL/min, the initial fracturing process created two symmetrical strain bands. The middle area had a smaller strain.
- During the TPF, cluster 4 fractured, clusters 2 and 3 did not fracture effectively; During the process of the cluster 4 fracture gradually closing, the cluster 1 fracture reopened.

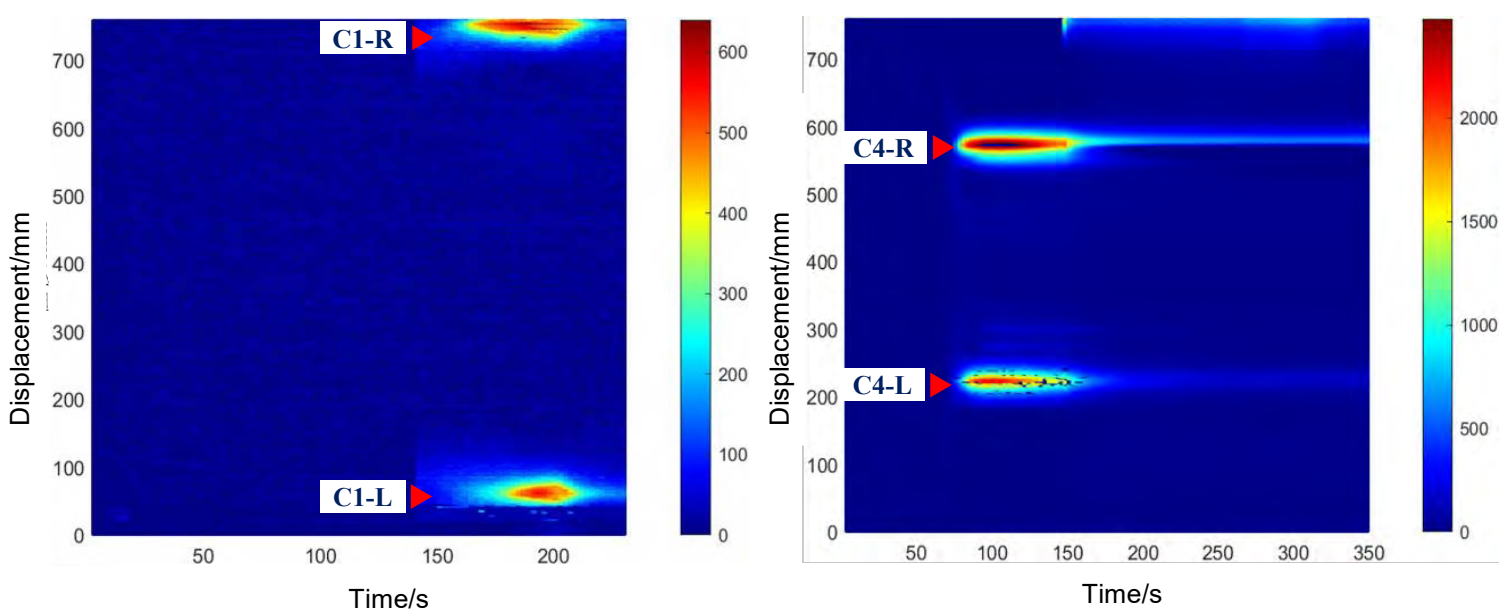

(a) before TPF (b) after TPF

Before and after the TPF of specimen 4, the 2# optical fiber waterfall diagram

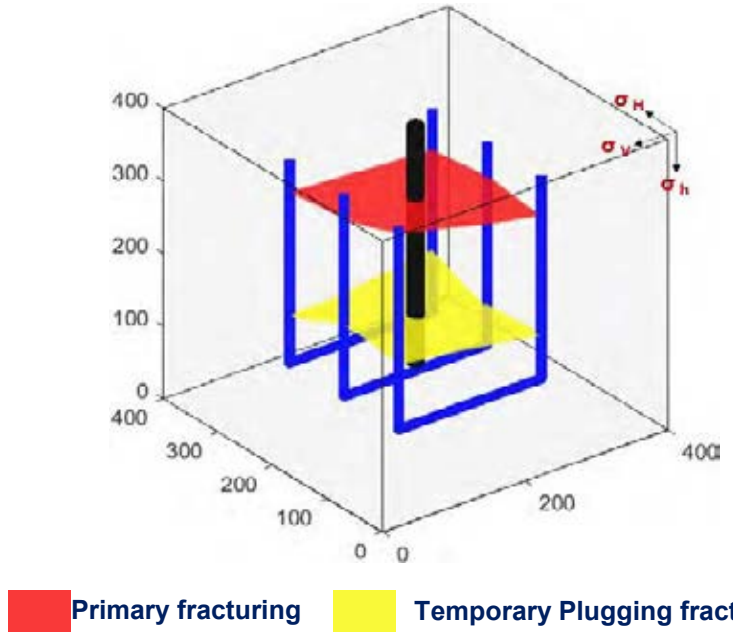

Reconstruction of fracture displacement

Parameters: Q=50mL/min, 4 clusters, d_c=5cm, $\Delta\sigma$=15MPa, 6mm TP fiber

4. Temporary Plugging Fracturing Experiment

(2) Specimen 5#

Parameters: Q=30mL/min, 4 clusters, d_c=5cm, $\Delta\sigma$=15MPa, 6mm TP fiber

- At a pumping rate of 30 mL/min, the initial fracturing pressure was **6.61 MPa**, the TPF pressure was **49.16 MPa**, with an increase of 643.70%.
- The initial fracturing only initiated the first fracture cluster; the TPF initiated the fourth fracture cluster, forming transverse fractures. At the same time, the third fracture cluster formed a longitudinal fracture parallel to the wellbore, which turned direction when it extended towards the wellhead and reached the second fracture cluster.

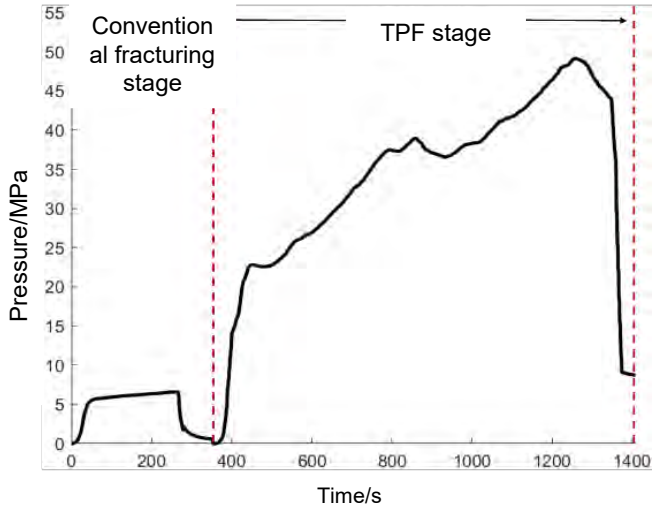

Specimen 5#'s full-process pumping pressure curve

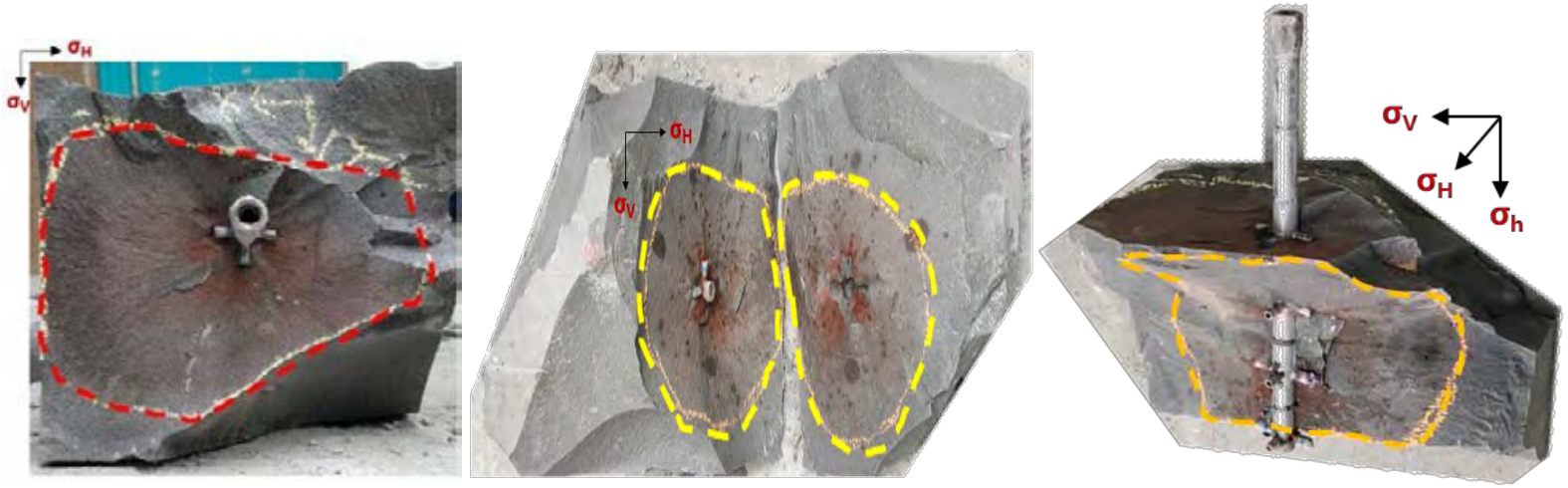

(a) The first cluster of fracture (b) The fourth cluster of fracture (c) The longitudinal fracture between the first to fourth clusters

Specimen 5#'s hydrological fracture morphology

4. Temporary Plugging Fracturing Experiment

- During the initial fracturing process, the strain changes throughout the entire fiber area were relatively small, with only slight strains occurring at the beginning and end of the fiber. It is speculated that only the first cluster formed a cross-cutting crack with insufficient extension.
- During the TPF, cluster 4 fractured. However, only one end of this fracture extended to the optical fiber. This indicates that the fracture in cluster 4 is an asymmetric extension fracture.

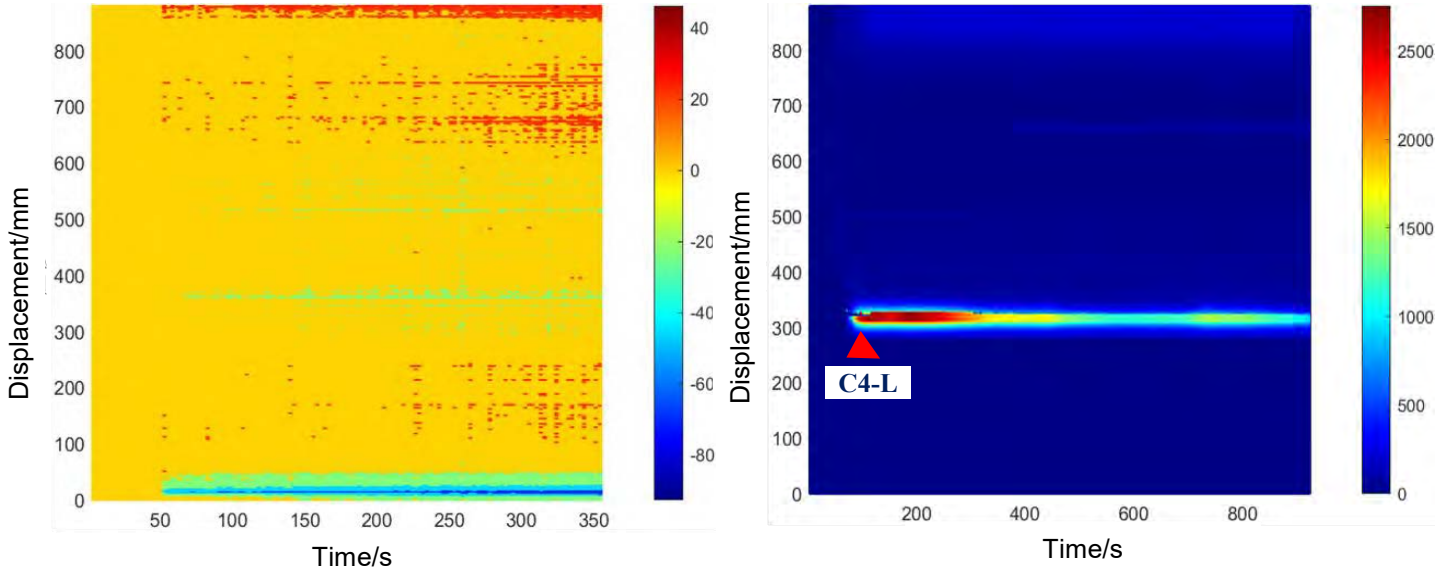

(a) before TPF (b) after TPF

Before and after the TPF of specimen 5, the 2# optical fiber waterfall diagram

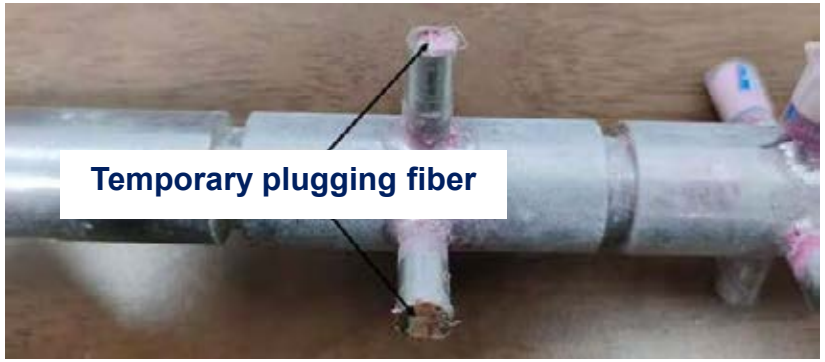

Accumulation morphology of temporary plugging fibers at the fracture mouth

Parameters: Q=30mL/min, 4 clusters, d_c=5cm, $\Delta\sigma$=15MPa, 6mm TP fiber

4. Temporary Plugging Fracturing Experiment

(3) Specimen 6#

Parameters: Q=20mL/min, 4 clusters, d_c=5cm, $\Delta\sigma$=15MPa, 6mm TP fiber

- At a pumping rate of 20 mL/min, the initial fracturing pressure was **8.09 MPa**, the TPF pressure was **13.77 MPa**, with an increase of 70.20%.
- The first fracture initiation cluster 1; Under low flow rate, the temporary plug fibers failed to effectively seal the fractures of cluster 1, but they caused the fractures of cluster 1 to change direction.

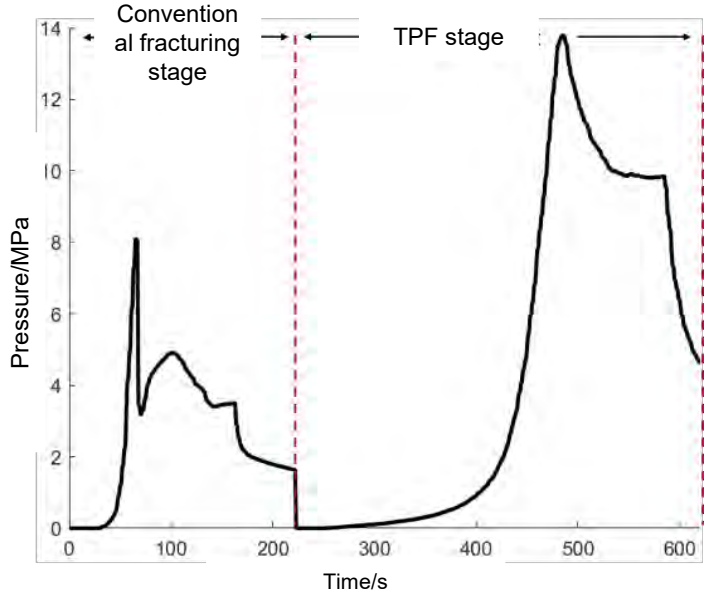

Specimen 6#'s full-process pumping pressure curve

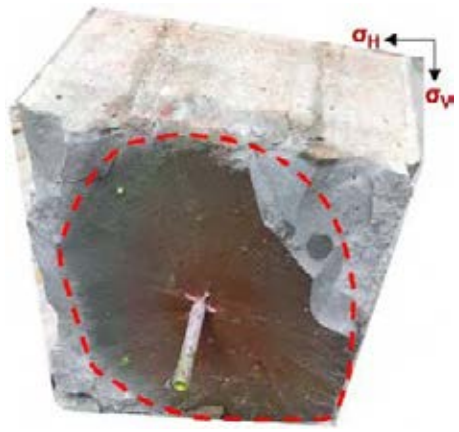

(a) The first cluster of fracture

(b) The first cluster of steering fractures

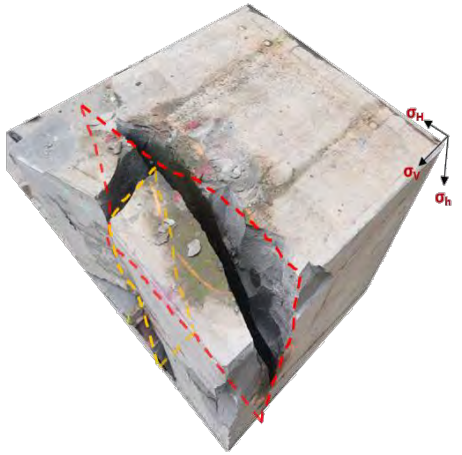

(c) The complete morphology of fractures in rock specimen

Specimen 6#'s hydrological fracture morphology

4. Temporary Plugging Fracturing Experiment

- **The initial fracturing** resulted in strain bands at the beginning and end of the U-shaped support, indicating that perforation **cluster 1** initiated the fracture.
- During the TPF, the strain zone appears at the location where the initial fracturing caused strain.

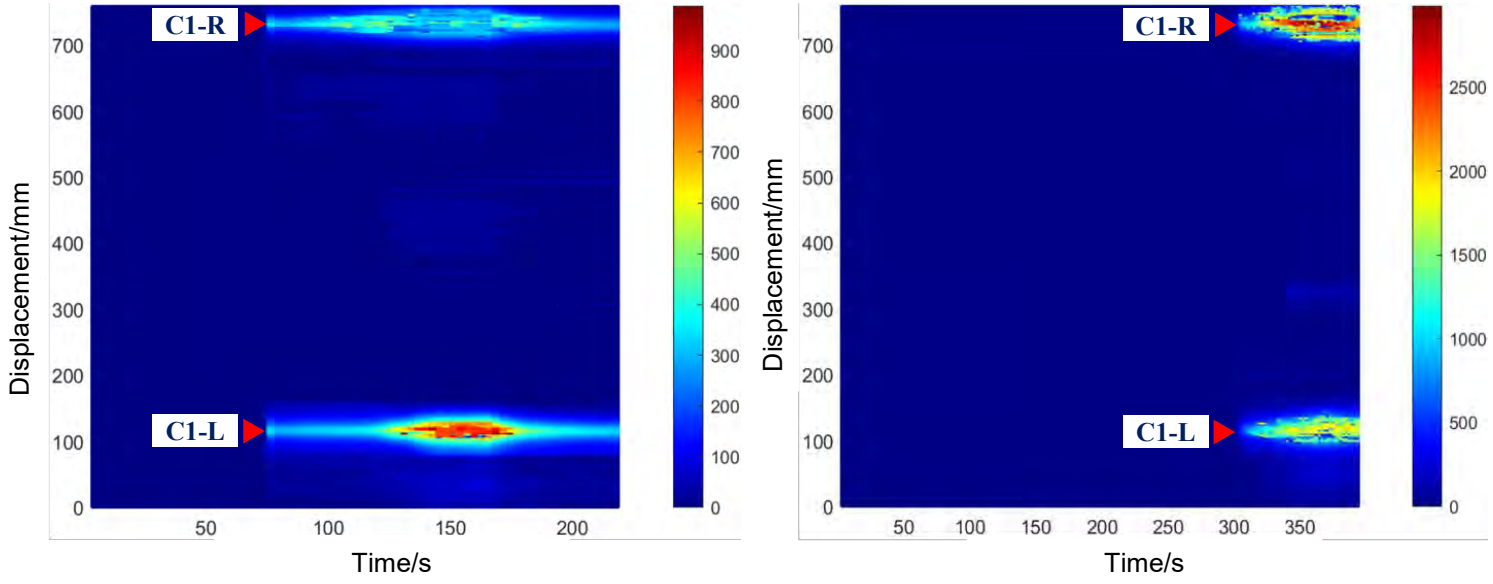

(a) before TPF

(b) after TPF

Before and after the TPF of specimen 6, the 2# optical fiber waterfall diagram

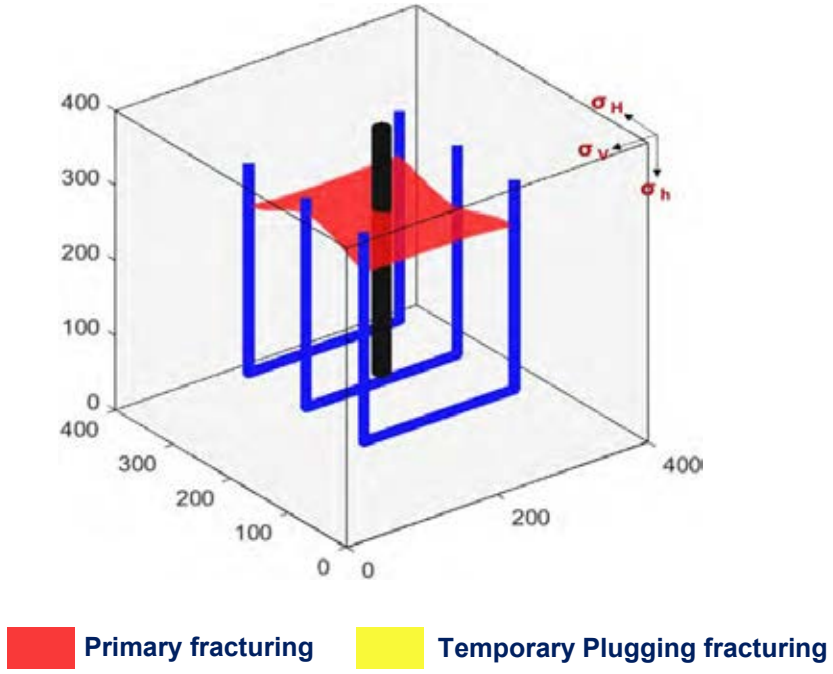

Reconstruction of fracture displacement

Parameters: Q=20mL/min, 4 clusters, d_c=5cm, $\Delta\sigma$=15MPa, 6mm TP fiber

4. Temporary Plugging Fracturing Experiment

(4) Discussion

- Under low pumping rate conditions (20 mL/min), it is difficult to form an effective plugging for the opened perforation clusters. However, with high injection speed (30 mL/min, 50 mL/min), the fracturing fluid can enhance its carrying capacity for the temporary plugging agent fibers.

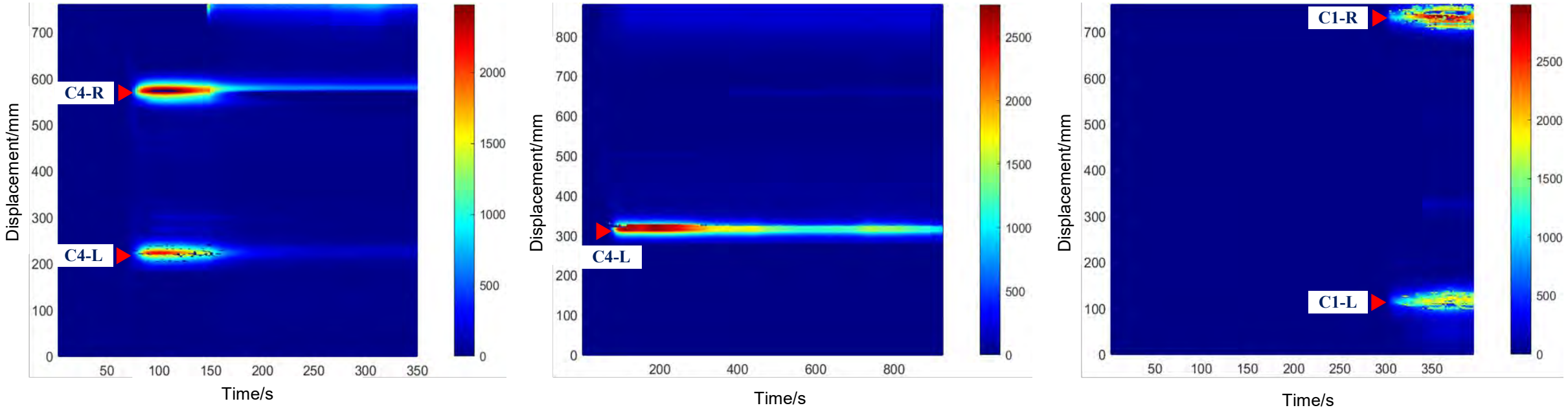

The fracture extensions of TPF

4. Temporary Plugging Fracturing Experiment

4.4 HF geometry and fiber response under different Δσ

(1) Specimen 7#

Parameters: Q=30mL/min, 5 clusters, d_c=5cm, $\Delta\sigma$=12MPa, 70/140 TP particle

- The initial fracturing pressure was **15.90 MPa**. During the TPF stage, after multiple pressure fluctuations, it rose to the fracture pressure of **28.68 MPa**, with an increase of 80.38%.
- During the initial fracturing, fluid was injected into the **first**, **second**, **fourth** and **fifth** clusters of perforations. After the TPF, the fractures all slightly **deviated towards the wellhead direction**.

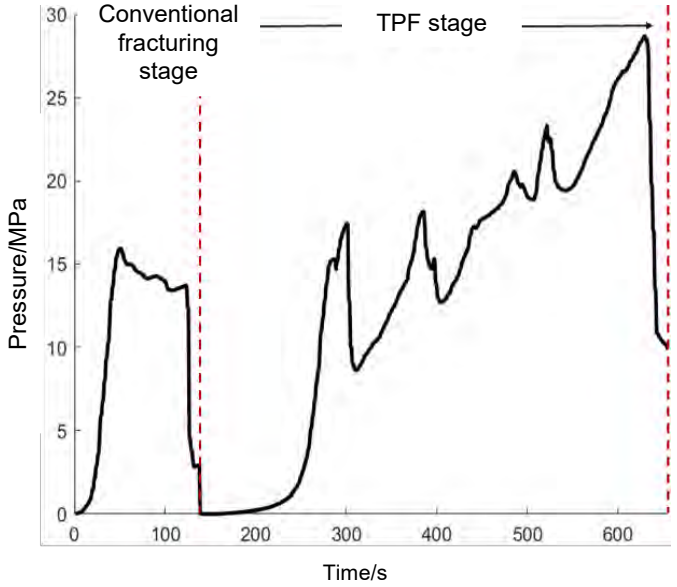

Specimen 7#'s full-process pumping pressure curve

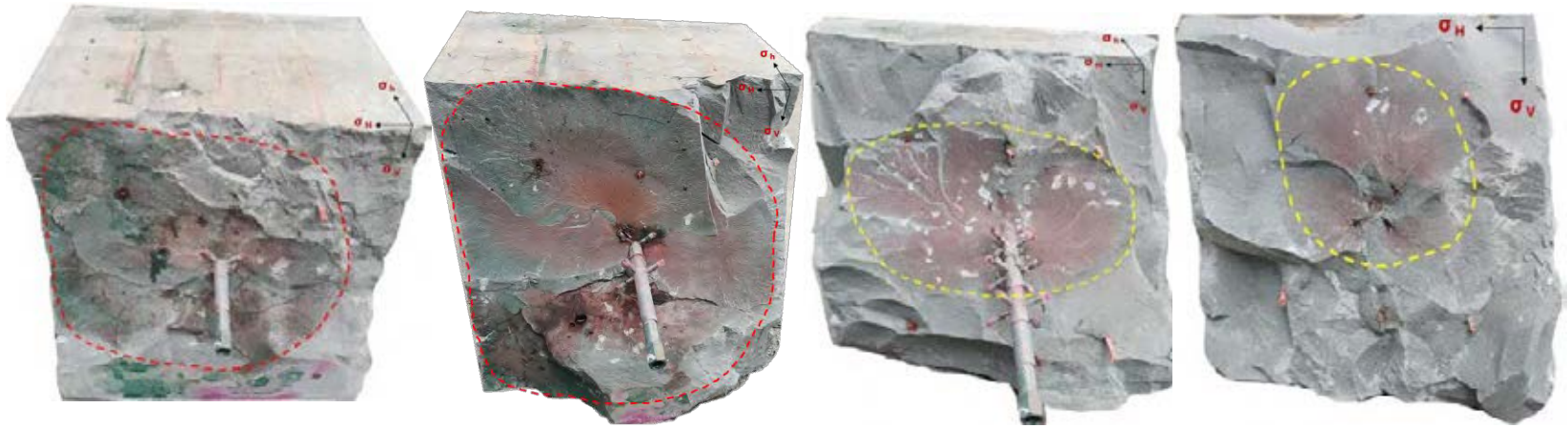

(a) The first cluster of fracture

(b) The second cluster of fracture

(c) The fourth cluster of fracture

(d) The fifth cluster of fracture

Specimen 7#'s hydrological fracture morphology

4. Temporary Plugging Fracturing Experiment

- **The initial fracturing of the U-shaped support at the front end resulted in a strain band. However, no strain band appeared at the rear end, suggesting that the cluster 1 expanded on one side.**
- **During the TPF stage, the fiber waterfall diagram revealed multiple asymmetric strain bands, indicating that the temporary plugging process created multiple new fractures.**

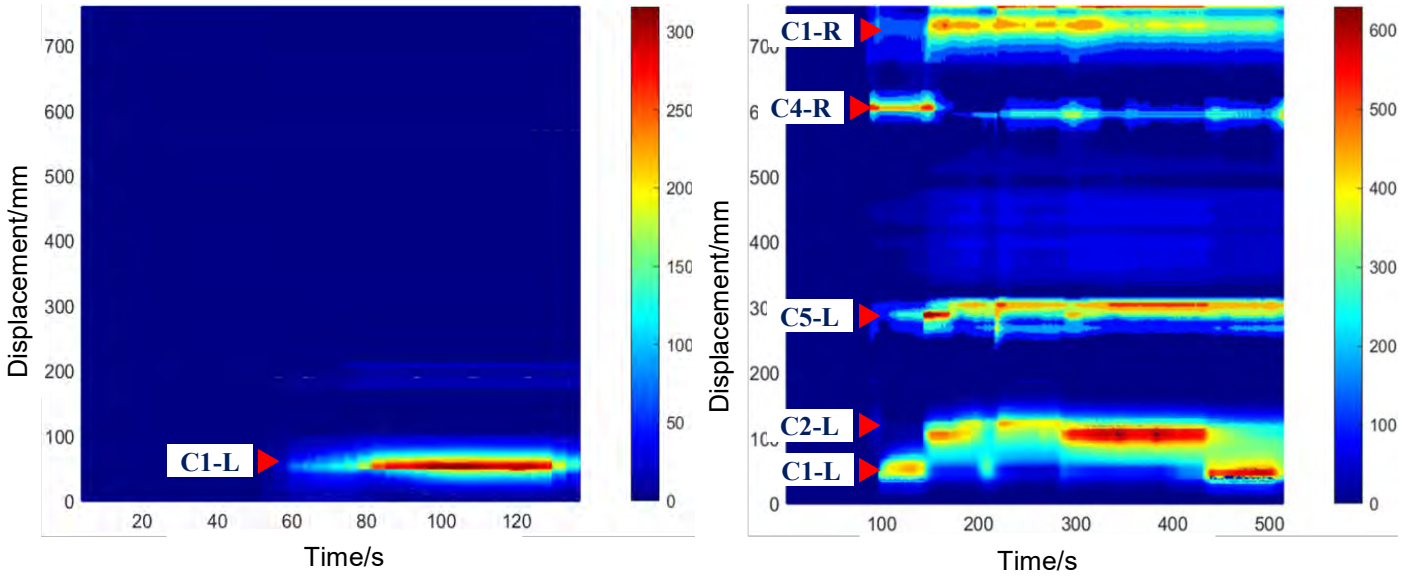

(a) before TPF (b) after TPF

Before and after the TPF of specimen 7, the 2# optical fiber waterfall diagram

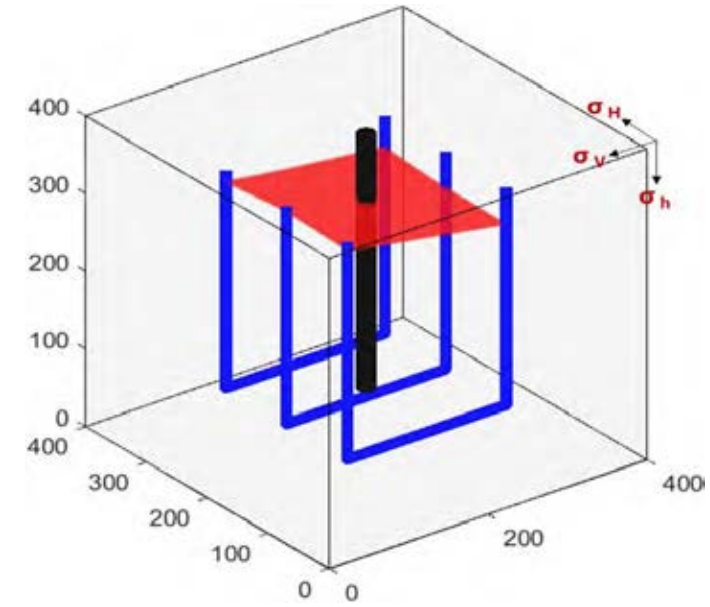

Reconstruction of fracture displacement

Parameters: Q=30mL/min, 5 clusters, d_c=5cm, $\Delta\sigma$=12MPa, 70/140 TP particle

4. Temporary Plugging Fracturing Experiment

(2) Specimen 8#

Parameters: Q=30mL/min, 5 clusters, d_c=5cm, $\Delta\sigma$=15MPa, 70/140 TP particle

- Initial fracturing pressure was **6.81 MPa**, resulting in two pressure peaks; the TPF pressure was **13.08 MPa**, with an increase of 92.07%.
- **The initial fracturing** opened the first and fifth clusters of perforations, the **TPF** opened the second cluster of perforations in the rock specimen. All three fractures were transverse cuts perpendicular to the wellbore.

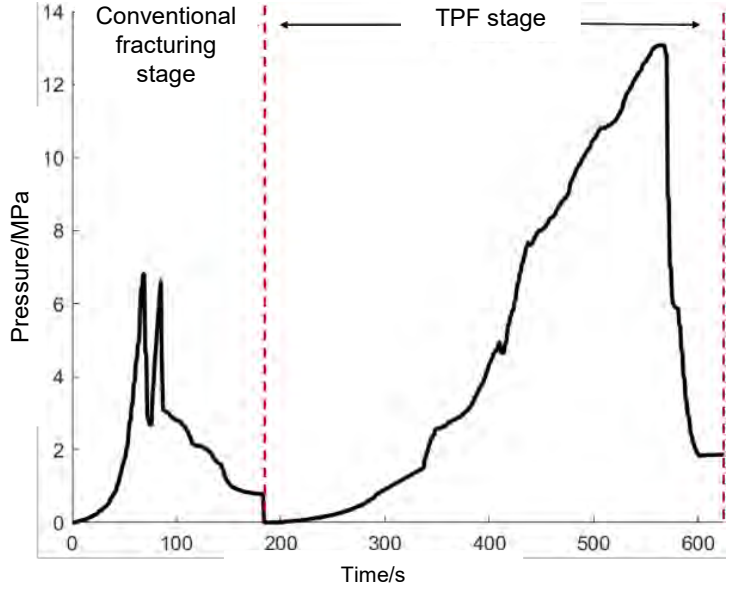

Specimen 8#'s full-process pumping pressure curve

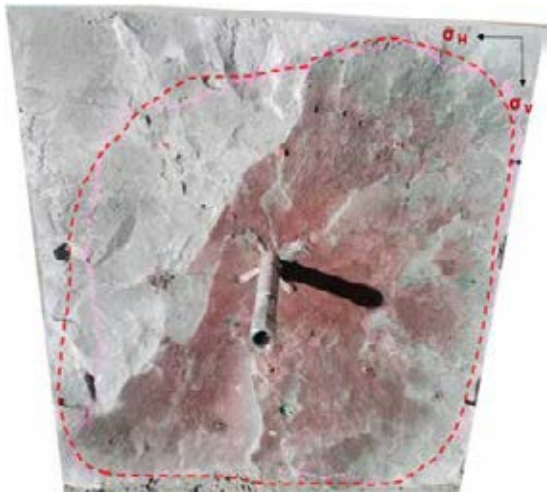

(a) The first cluster of fracture

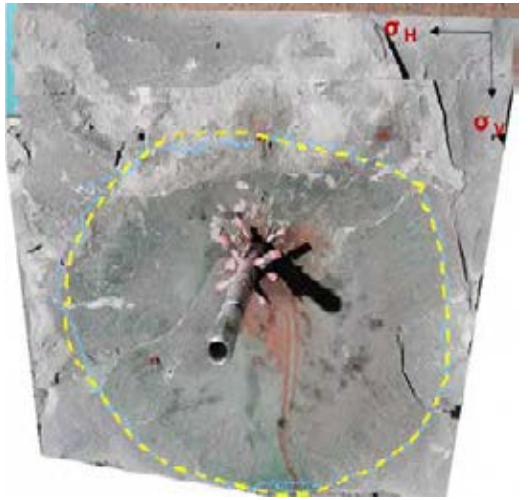

(b) The second cluster of fracture

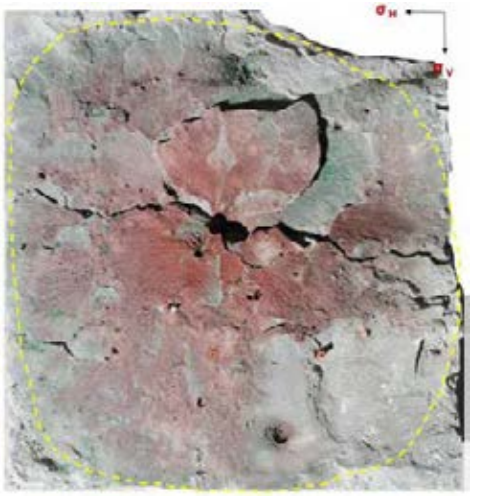

(c) The fifth cluster of fracture

Specimen 8#'s hydrological fracture morphology

4. Temporary Plugging Fracturing Experiment

(3) Specimen 9#

Parameters: Q=30mL/min, 5 clusters, d_c=5cm, $\Delta\sigma$=18MPa, 70/140 TP particle

- The initial fracturing pressure was **5.25 MPa**. The temporary plugging fracturing pressure first reached **4.92 MPa** and then gradually increased. It is speculated that the **temporary plugging particles have clogged the wellbore**.
- Cluster 1 developed a **transverse fracture** perpendicular to the wellbore. Due to the deposition of temporary sealing particles inside the wellbore, failed to achieve an **effective plugging**.

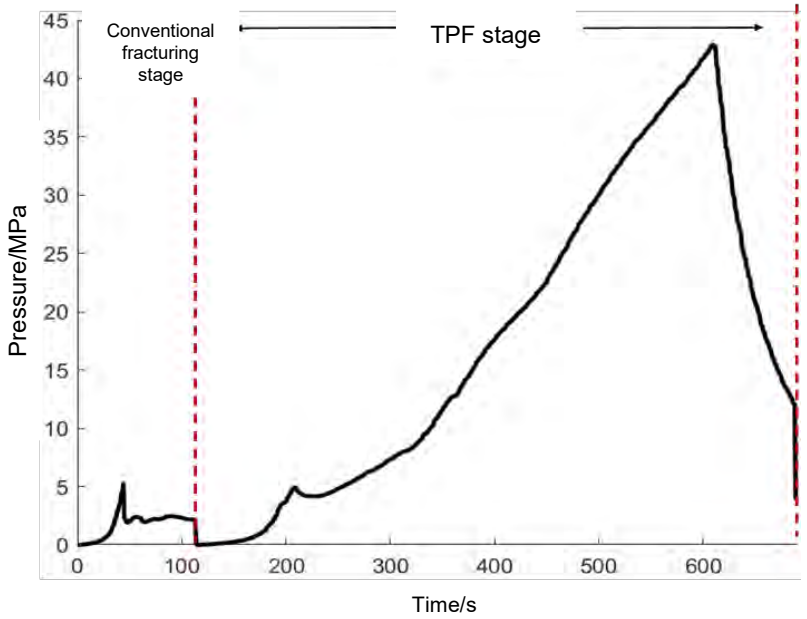

Specimen 9#'s full-process pumping pressure curve

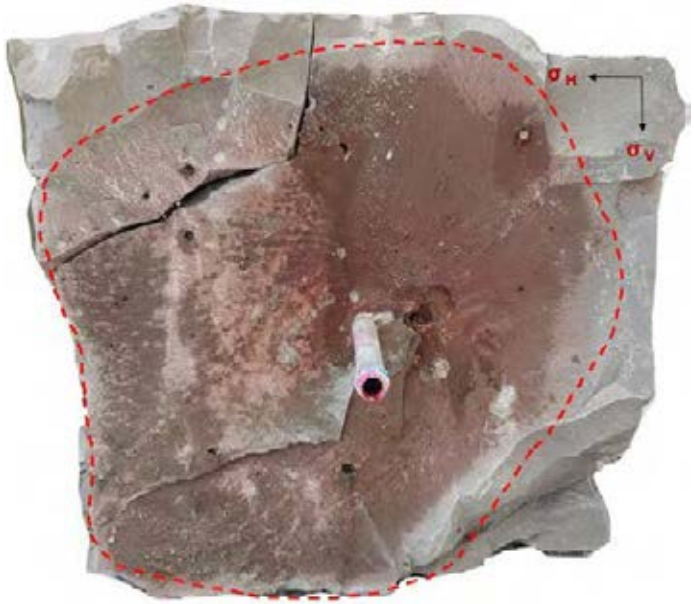

Specimen 9#'s hydrological fracture morphology

4. Temporary Plugging Fracturing Experiment

- During the initial fracturing, a strain band appeared at the front of the U-shaped support, indicating that the initial fracturing cluster 1 had initiated fracture propagation.
- During the TPF stage, no new strain bands appeared on the fiber waterfall diagram, indicating that TPF failed to create new fractures, and fracturing fluid flowed along the cluster 1 fractures.

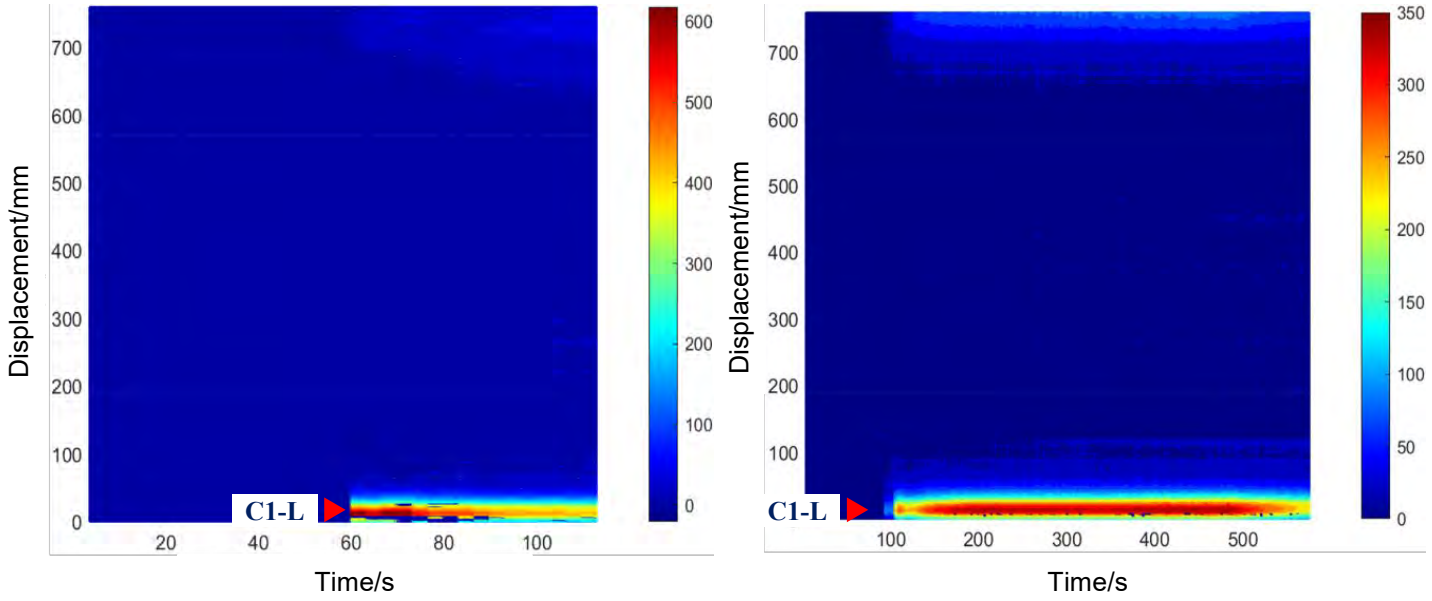

(a) before TPF (b) after TPF

Before and after the TPF of specimen 9, the 2# optical fiber waterfall diagram

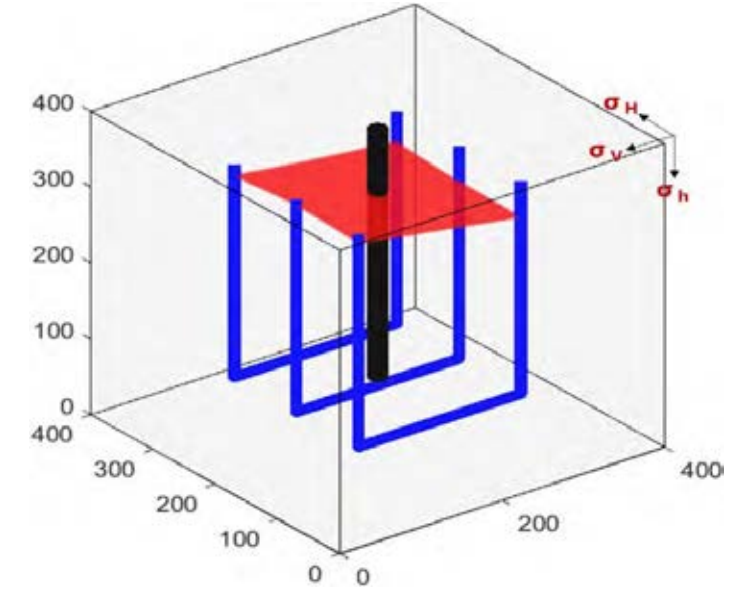

Primary fracturing Temporary Plugging fracturing

Reconstruction of fracture displacement

Parameters: Q=30mL/min, 5 clusters, d_c=5cm, $\Delta\sigma$=18MPa, 70/140 TP particle

4. Temporary Plugging Fracturing Experiment

(4) Discussion

- As the stress difference **increases**, the difficulty of initiating new fractures by TPF **increases**, the number of initiated new fractures **decreases**.

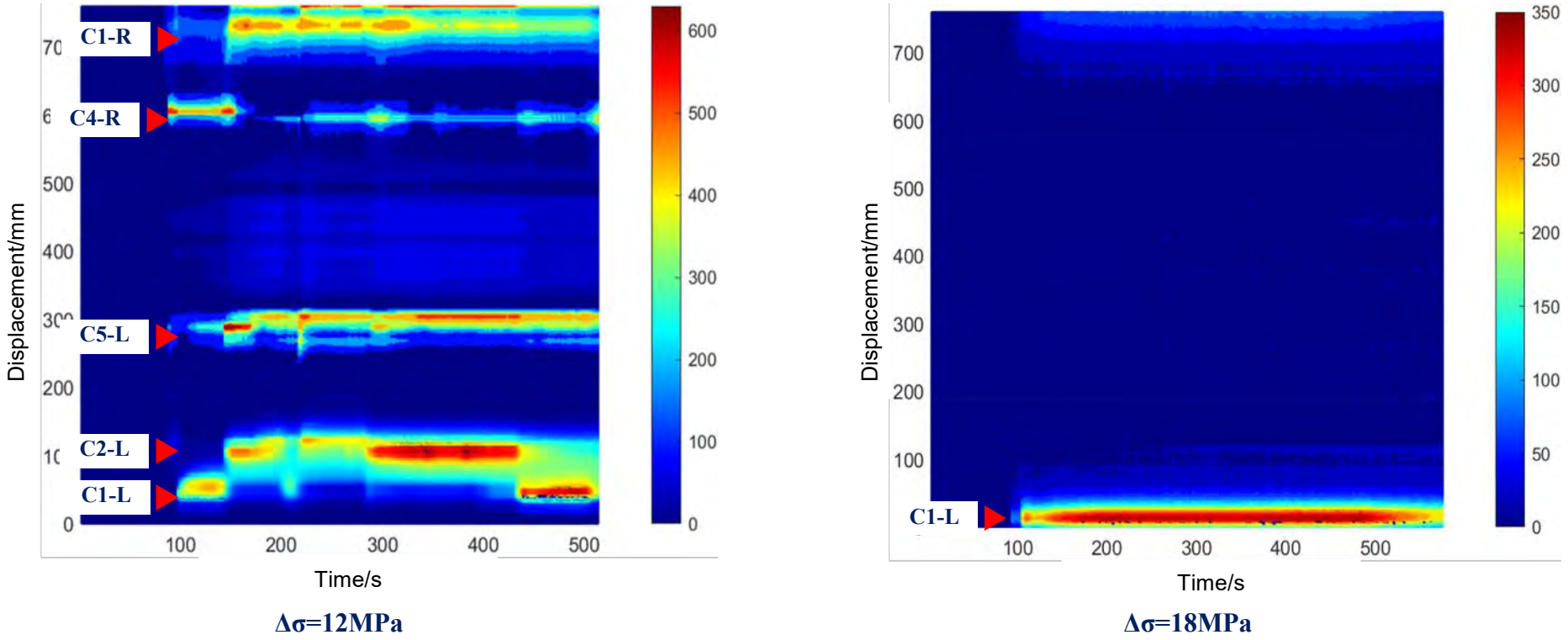

The fracture extensions of TPF

Content

5. Ongoing Novel Experiments

5.1 Multi-well three-dimensional fracturing physical simulation experiment

- Prepare a 400mm×400mm×400mm specimen and drill 5 horizontal wells with staggered distribution, which are arranged in upper, middle and lower three layers;
- Combined with the AE, distributed optical fiber strain monitoring system and strain gauge analysis system, monitor the fracture stress conduction path during multi-well fracturing to reveal the interwell stress interference mechanism and the connected morphology of interwell fractures.

Specimen processing scheme

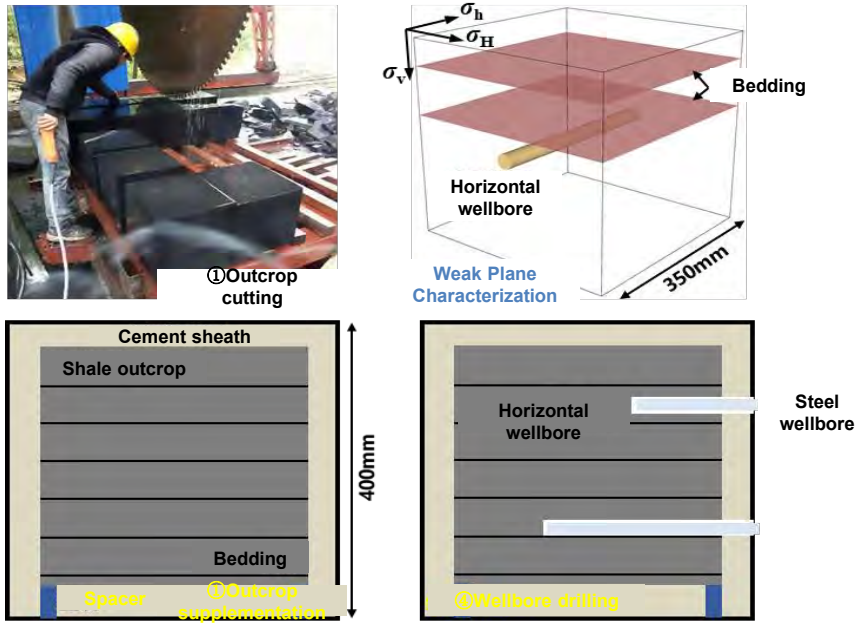

Three-dimensional fracturing wellbore drilling scheme

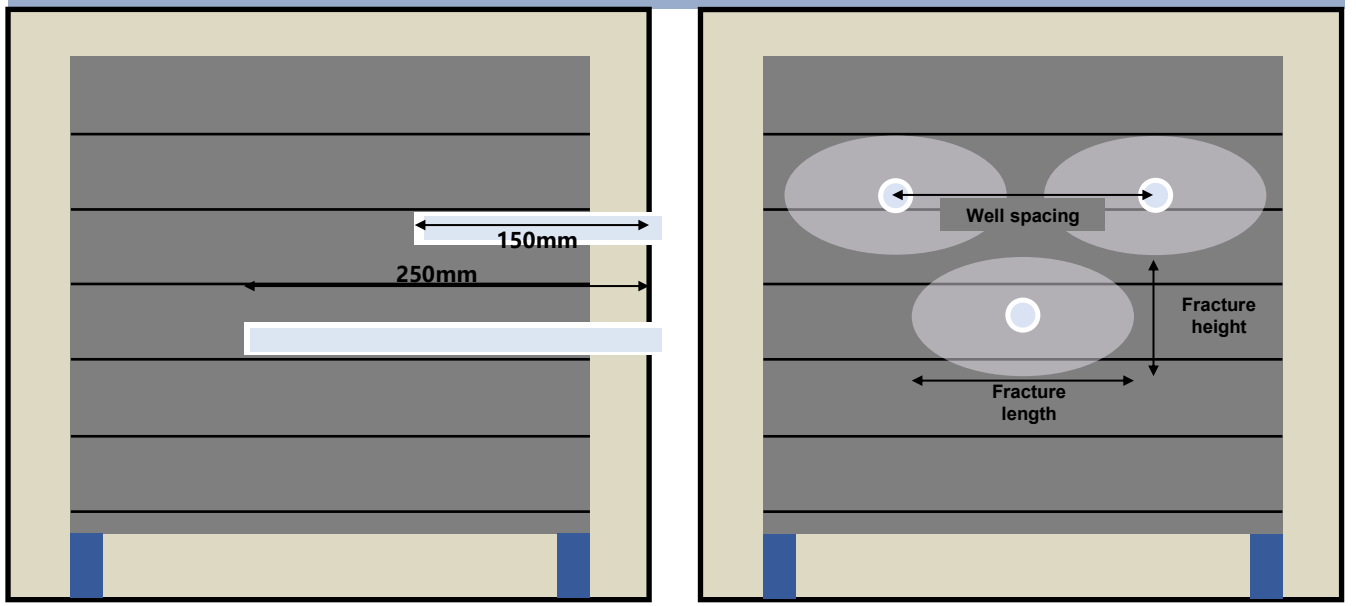

Side view of wellbore drilling

Front view of wellbore drilling

5. Ongoing Novel Experiments

5.2 Laboratory experiment on physical modeling of hydraulic fracturing for infill wells considering non - uniform pore pressure distribution

- Fabricate a square plate-shaped specimen with dimensions of 400 mm × 400 mm × 20 mm, pre-set natural fractures, drill three wellbores in the plate-shaped specimen.
- Inject fluid into two of the wellbores to simulate the fracture propagation process of pre-existing wells. Subsequently, extract fluid from these two wellbores to mimic the production phase of the pre-existing wells. Finally, inject fluid into the remaining wellbore.

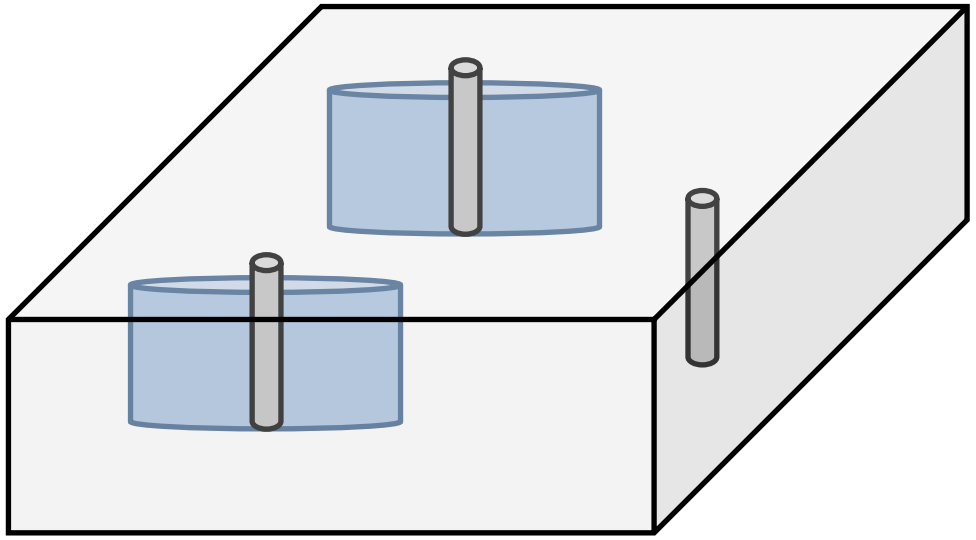

Hydraulic fracturing and fluid extraction from old wells to simulate a non-uniform pore pressure field

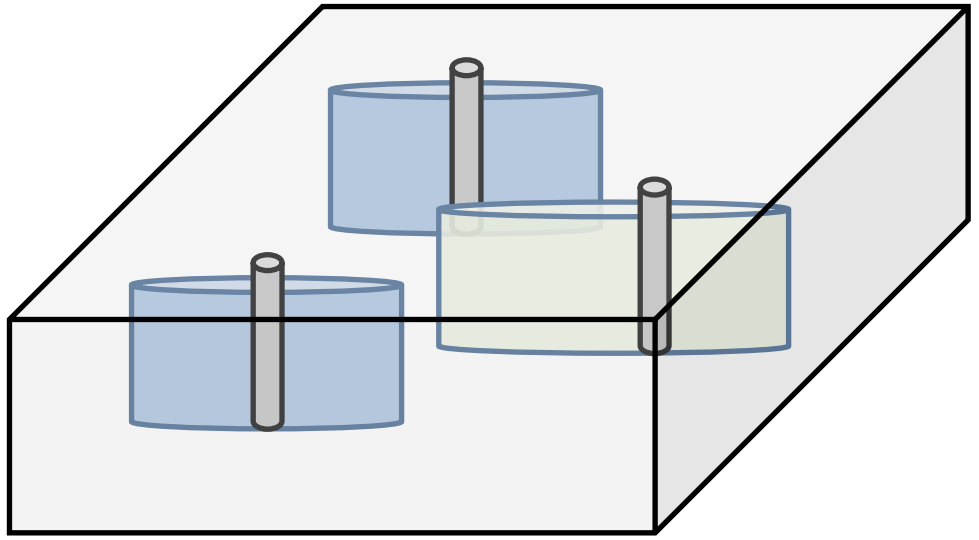

Hydraulic fracturing crack propagation of infill wells under non-uniform pore pressure fields

5. Ongoing Novel Experiments

5.3 True Triaxial Experiment on Fault Slip Induced by Fracturing Stress

- A physical simulation of stress transfer during fracturing is performed. Perforation eyes are located near the fault plane, enabling fracturing fluid to enter the fault and cause its slip;
- **Eight strain gauges** are arranged on the fault surface. Strain gauges are used to monitor the slip characteristics of the fault plane. Meanwhile, a high-frequency acoustic probe is used to monitor fracturing AE signals, and a low-frequency acoustic probe is used to monitor slip signals.

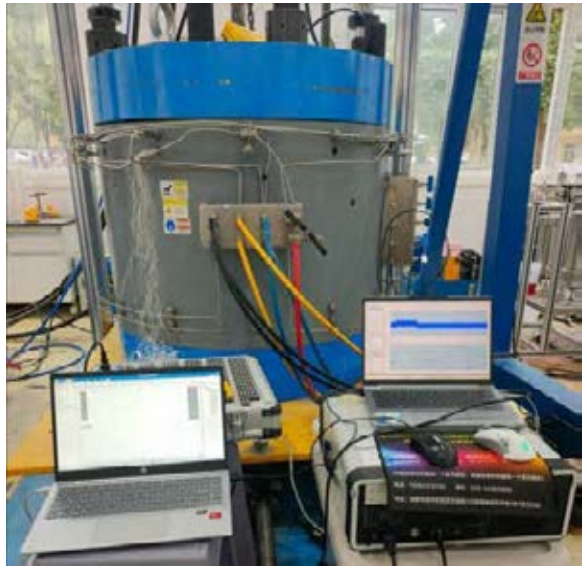

hydraulic fracturing fault activation physical modeling experimental system

cast rock samples

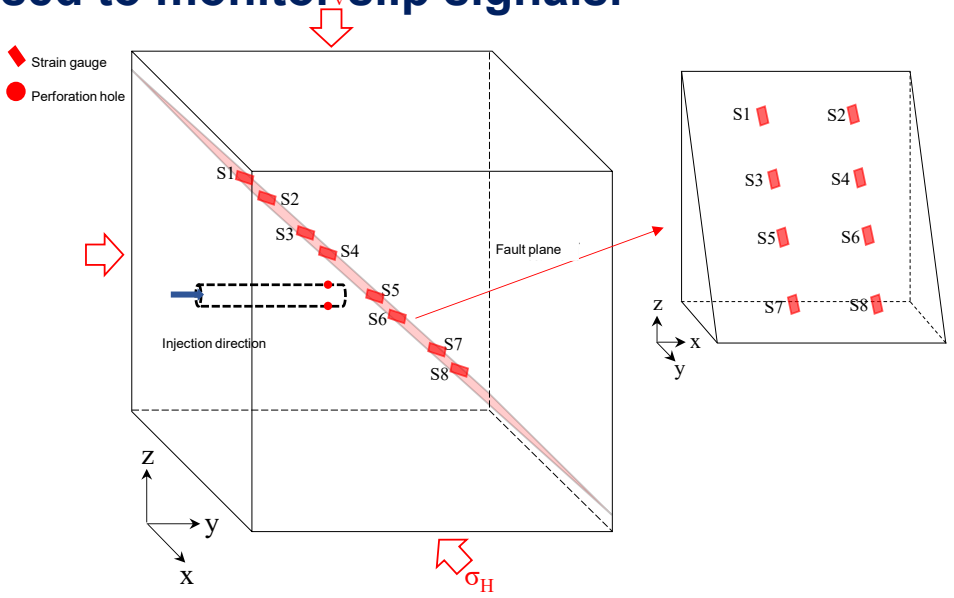

schematic diagram of strain gauge installation on fault surface

Thanks for listening!

Email：zhuhaiyan040129@163.com